Ann. Rev. Nucl. Sci. 1977. 27: 1–35
Copyright © 1977 by Annual Reviews Inc. All rights reserved

ANNUAL REVIEWS Further
Quick links to online content

Annu. Rev. Nucl. Sci. 1977.27:1-35. Downloaded from www.annualreviews.org
Access provided by 2409:4070:4701:c29b:fcdc:51af:e256:c850 on 09/30/22. For personal use only.

SPONTANEOUSLY FISSIONING ISOMERS

*5580

R. Vandenbosch[1]
Department of Chemistry, University of Washington, Seattle, Washington 98195

CONTENTS

INTRODUCTION 1
STATIC PROPERTIES 3
Isomer Excitation Energies 3
Barrier Heights 3
Comparison of Excitation Energies and Barrier Heights with Theoretical Potential Energy Surfaces 4
Spins and Moments 6
Spin-dependence of projectile-fragment angular correlations 6
Nuclear g-factors 11
Moments of inertia 13
Quadrupole moments 15
DECAY PROPERTIES 17
Half-Lives and Barrier Penetrabilities 17
Branching Ratios 23
Fragment Kinetic Energy and Mass Distributions for Isomeric Fission 26
EXCITATIONS OF SHAPE ISOMERS 27
Rotational Excitations 27
Vibrational Excitations 28
Single-Particle Excitations 29
Odd-A nuclei 29
Two-quasiparticle excitations 30
CONCLUSION 32

INTRODUCTION

In 1962 the first report (1) on the observation of a spontaneously fissioning species with an anomalously short lifetime appeared. Further work revealed that the excitation energy of one of these isomers was about 3 MeV and that its spin was considerably lower than the value required to account for the necessary γ-ray retardation in terms of a spin-forbiddenness effect. A number of different isomers were characterized and a systematics of the half-lives began to emerge. These developments led to increased interest in the idea that spontaneous-fission isomers were actually

[1] Work supported in part by US Energy Research and Development Administration.

shape isomers, corresponding to a second minimum in the potential energy along the elongation degree of shape deformation. A schematic representation of such a potential energy function is given in Figure 1, where we define a few of the quantities used throughout this review.

A very significant theoretical development was taking place concurrently with the experimental characterization of shape isomers. This development had its origins partly in an attempt to understand the nature of single-particle effects on nuclear binding energies (2) and partly in the failure of early purely microscopic calculations to give a reasonable description of the potential energy at large deformations. In a macroscopic-microscopic approach as first developed by Strutinsky (3,4), the smooth trends of the potential energy with respect to particle numbers and deformation are taken from a macroscopic (liquid-drop) model and the local fluctuations due to quantization of the single-particle motion are taken from a microscopic (single-particle) model. The latter fluctuations are sometimes designated the shell corrections and the method of calculating the potential energy is known as the shell-correction method. The second minimum in the potential energy curve for certain actinide nuclei is found to result from a superposition of a second minimum in the shell correction with the relatively flat maximum in the macroscopic part of the deformation energy.

In addition to providing an understanding of the origin of the anomalous spontaneous-fission lifetimes, the double-humped barrier also provided an explanation for some previously puzzling features of induced fission. Resonant-like structure in sub-barrier fission-excitation functions could now be attributed to transmission resonances associated with the dependence of the penetration of a double-humped fission barrier on energy. Intermediate structure observed in low-energy neutron-induced resonance studies could be attributed to coupling of the more numerous states in the first well with the smaller number of states correspond-

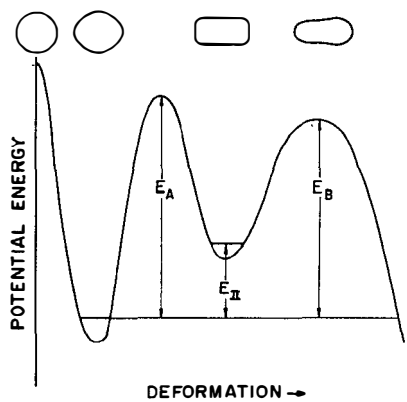

Figure 1 Schematic view of double-humped barrier and of nuclear shapes at selected deformations.

Annu. Rev. Nucl. Sci. 1977.27:1-35. Downloaded from www.annualreviews.org
Access provided by 2409:4070:4701:c29b:fcdc:51af:e256:c850 on 09/30/22. For personal use only.

ing to excitation of the shape isomer. Anomalies in the level densities for deformations corresponding to the inner and outer barriers were identified with the breaking of certain symmetries of the nuclear shape (5).

In this review we concentrate on the experimental information relating to the properties of shape isomers. We do not attempt to provide a comprehensive review of theoretical developments, but primarily draw only on the results of these investigations as they bear on the experimental observations. For fairly recent summaries of theoretical aspects of this subject, the reader is referred to the papers of Brack et al (6), Pauli (7), and Möller & Nix (8). We also do not discuss in much detail resonance effects in near-barrier induced fission. The Proceedings of the 1973 IAEA Symposium on the Physics and Chemistry of Fission (9) provide valuable references concerning all of these aspects. A fairly recent review (10) and a book (11) discuss shape isomerism, as well as other aspects of nuclear fission.

Annu. Rev. Nucl. Sci. 1977.27:1-35. Downloaded from www.annualreviews.org
Access provided by 2409:4070:4701:c29b:fcdc:51af:e256:c850 on 09/30/22. For personal use only.

STATIC PROPERTIES

Isomer Excitation Energies

The excitation energy E_{II} of the isomeric state relative to the ground state is usually obtained from the threshold behavior of the excitation function for isomer production. Most of the measurements are performed using reactions in which two or more neutrons are emitted prior to reaching the nucleus of interest, leading to appreciable slopes of the excitation functions near threshold. Thus an extrapolation from the lowest energy at which measurements are made to the threshold energy is required. A statistical model is employed to guide this extrapolation, and an absolute accuracy of perhaps 0.3 MeV can be achieved. A considerable body of data has been analyzed by Britt and co-workers (12). Values between 1.6 and 2.6 MeV have been obtained for a number of plutonium, americium, and curium isomers. (We exclude from discussion here excitation energies of isomers believed to be excited states of shape-isomeric nuclei; see discussion in section on Excitations of Shape Isomers.) One very precise isomer excitation energy, 2.56 MeV, is known from the observation of the γ decay branch from the ^{238}U isomeric state back to the ground state (13). Unfortunately, this isomer cannot be populated in reactions suitable for threshold measurements and hence a quantitative test of the statistical model analyses is not possible.

Barrier Heights

It is of considerable interest to characterize the inner and outer barriers that support the isomeric states. The height of the highest of the two barriers can usually be determined fairly easily from prompt fission–probability excitation functions. If transmission resonances (see section on Vibrational Excitations) are observed, then information about both barriers can be obtained. Additional information comes from analysis of isomer excitation functions. Back and co-workers (14, 15) have performed a very comprehensive statistical model analysis of fission-probability distributions for nuclei of actinide elements from thorium through californium. The model takes into account competition between fission, neutron, and γ emission in the decay of the

compound nucleus. It uses resonant fission penetrabilities for a double-humped fission barrier, with damping of the resonances accomplished by introducing an imaginary component in the potential at the position of the second well. The results of analyses with this model are shown in Figure 2, where it is seen that the value of the height of the inner barrier E_A remains remarkably constant throughout this large range of Z and A. The height of the outer barrier E_B, however, decreases considerably as Z is increased.

Comparison of Excitation Energies and Barrier Heights with Theoretical Potential Energy Surfaces

The development by Strutinsky (3,4) of the macroscopic-microscopic method for calculating potential energy surfaces has made it possible to calculate fission barriers and isomer excitation energies that are in fairly good agreement with experimental trends. The basis of this method is to use a macroscopic model to determine the smooth trends of the potential energy with deformation and particle number, and a microscopic model to determine the fluctuations about these trends due to single-particle (shell) effects. The macroscopic model employed is the liquid-drop or liquid-droplet model.

A full exposition of the method is given in a review paper (6). There have been several tests of this method by comparison with Hartree-Fock calculations (16–18). The results seem to confirm the validity of the macroscopic-microscopic approach. Only one (18) of these calculations, however, attempted to reproduce the potential energy curve for a heavy nucleus exhibiting a double-humped barrier, and in this case only reflection symmetric shapes were considered. Thus, for the present one must rely on the results of the macroscopic-microscopic method when comparisons with experiment are attempted.

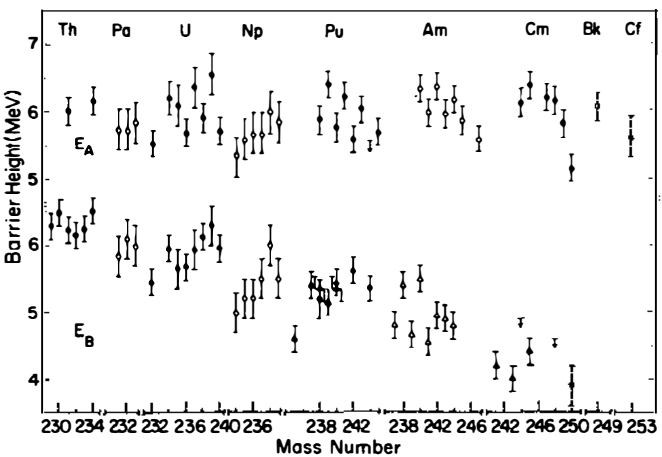

Figure 2 Fission-barrier heights obtained from fits to the fission probability distributions. Note the separate scales for the E_A and E_B values. From Back et al (15).

Annu. Rev. Nucl. Sci. 1977.27:1-35. Downloaded from www.annualreviews.org
Access provided by 2409:4070:4701:c29b:fcdc:51af:e256:c850 on 09/30/22. For personal use only.

Annu. Rev. Nucl. Sci. 1977.27:1-35. Downloaded from www.annualreviews.org
Access provided by 2409:4070:4701:c29b:fcdc:51af:e256:c850 on 09/30/22. For personal use only.

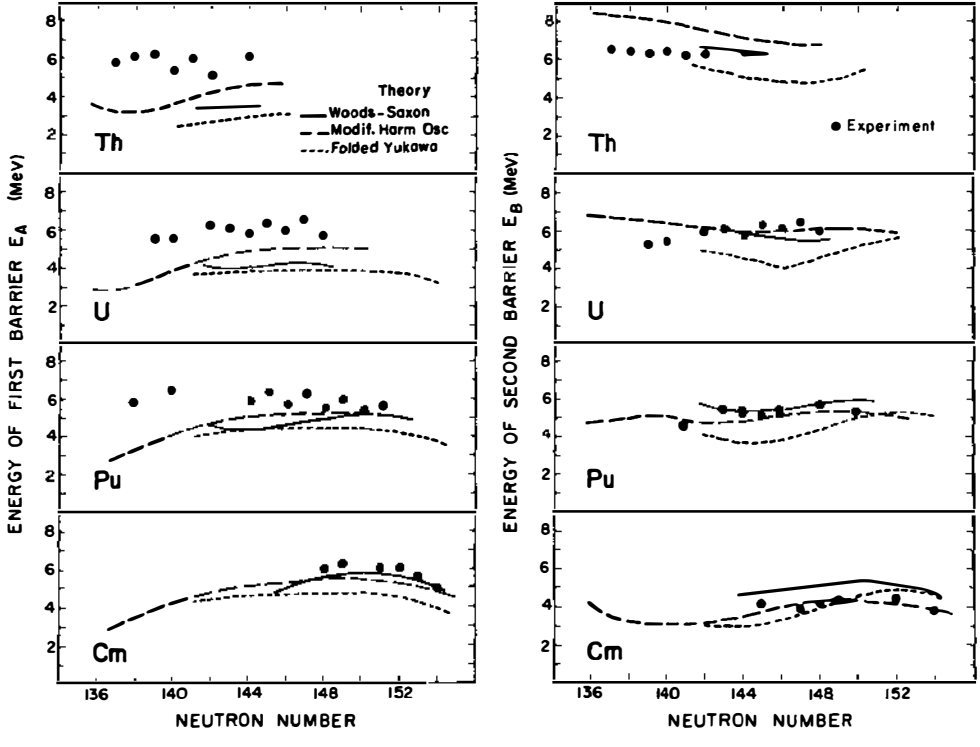

Figure 3 Measured heights of the first and second barrier as a function of neutron number and theoretical predictions from shell-correction calculations based on different single-particle potentials. After Specht (29), as updated by Metag. See Specht (29) for references to original work, except for the two new points for ^{232}Pu and ^{234}Pu, representing unpublished work of Metag et al (private communication).

The potential used in the macroscopic-microscopic method to generate the single-particle energies from which the shell and pairing corrections are derived may be of oscillator, Woods-Saxon. or folded Yukawa form. The shape parameterization must be general enough to describe the necking-in of the nuclear shape at the later stages, particularly at the second barrier. It has also been found that it is very important to include reflection-asymmetric shapes, as the outer barrier height E_B is lowered several MeV with inclusion of this degree of freedom (19–22). For the higher-Z actinides (Pu and beyond) a significant lowering of the inner barrier occurs when axially asymmetric degrees of freedom are included (23–26).

The most recent theoretical calculations (8, 27, 28) reproduce most of the important features of the observed dependencies of the inner and outer barriers on Z and A. Specht (29) has compared the results of several calculations with experimental results as shown in Figure 3. The decrease of the outer barrier height with increasing Z is in large measure due to the shift of the liquid-drop part of the barrier to smaller deformations, as illustrated by Metag (30) in Figure 4. The major anomaly revealed by the comparison between the calculated and experimental results in Figure 3 is that the height of the inner barrier is greatly underestimated in the theoretical calculations. One possible resolution of this anomaly has been suggested by Möller & Nix (8), who have found that for nuclei with small neutron numbers the outer barrier is split into two barriers, separated by a third minimum. They suggest that it is this third minimum that supports the transmission resonances observed (31), and that the analyses of the fission probabilities have located these two outer barriers, rather than the inner and outer barriers as assumed. It is not clear, however, that this suggestion can explain the discrepancy for heavier nuclei such as plutonium.

A previous (32) comparison of the experimental and theoretical isomer excitation energies is given in Figure 5. The theoretical calculations (8, 33, 34) give approximately the correct energies, except for the lighter elements, where the calculations of Möller & Nix (8) appear to seriously underestimate the energies.

Spins and Moments

SPIN DEPENDENCE OF PROJECTILE-FRAGMENT ANGULAR CORRELATIONS There have been several attempts to learn about the spins of specific isomeric states by studying

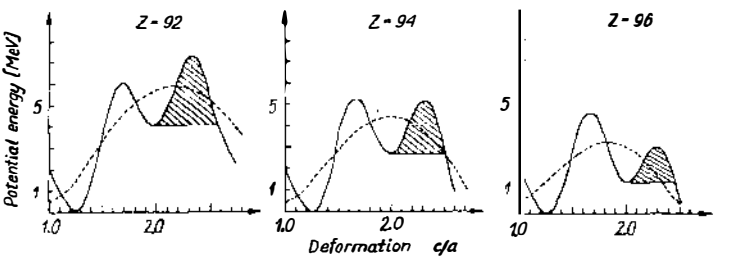

Figure 4 The influence of the liquid-drop part (*dashed curve*) of the double-humped fission barrier (*solid curve*) on the relative heights of the inner and outer barriers. From Metag (30).

Annu. Rev. Nucl. Sci. 1977.27:1-35. Downloaded from www.annualreviews.org
Access provided by 2409:4070:4701:c29b:fcdc:51af:e256:c850 on 09/30/22. For personal use only.

the angular distribution of fission fragments with respect to the beam (35–40). The principle of this method is that a reaction such as $\alpha, 2n$ is used to form compound nuclei with their angular momenta aligned in the plane perpendicular to the beam direction. The fragment anisotropy is then determined by the angular momentum I of the isomeric state and by the value of the projection of this angular momentum on the nuclear symmetry axis, K_B, at the second barrier. Here the usual assumption, confirmed in prompt fission studies, has been made that it is the available K bands at the barrier that determine the anisotropy. In the present circumstance of barrier penetration rather than over-the-barrier fission, the rationalization for this assumption is that the penetrability integral for each particular K-channel is most affected by the maximum in the potential energy curve for that channel, i.e. at the top of the barrier. Contributions from several K_B states cannot be excluded, although the

Annu. Rev. Nucl. Sci. 1977.27:1-35. Downloaded from www.annualreviews.org
Access provided by 2409:4070:4701:c29b:fcdc:51af:e256:c850 on 09/30/22. For personal use only.

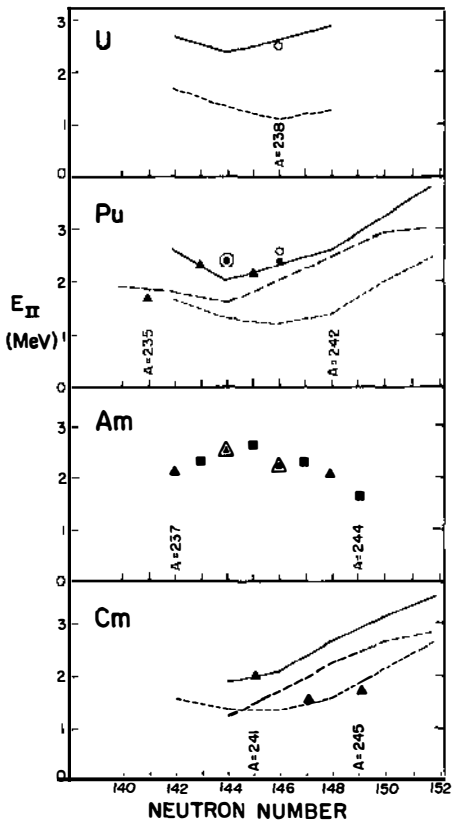

Figure 5 Comparison of experimental and theoretical excitation energies. The solid, long-dashed, and short-dashed lines are the theoretical results of Pauli & Ledergerber (33), Möller (34), and Möller & Nix (8). From (32).

exponential dependence of the penetrability on potential energy will usually result in the lowest state dominating. The fragment angular distribution for fission from a state with angular momentum I and projection K_b can be written (35) as

$$W_{K_b}^{I}(\theta) = \sum_{\lambda} A_\lambda G_\lambda(t) P_\lambda(\cos\theta), \qquad \lambda = 0, 2, \ldots, 2I \qquad 1.$$

with

$$A_\lambda = \frac{2I+1}{2} \sum_{M} (-1)^{K_b - M} f(M) C^{II\lambda}_{-MMO} C^{II\lambda}_{-K_b K_b O}. \qquad 2.$$

In these expressions, P_λ are the Legendre polynomials, the C are Clebsch-Gordan coefficients, the $f(M)$ the occupation probabilities of the magnetic substates M of the spin relative to the beam axis, and the $G_\lambda(t)$ the attenuation factors for any perturbation of the correlation by extranuclear fields. A summary of the available data on the experimental ratios of $W(\theta)/W(90°)$ is given in Table 1. We note that the mere existence of an anisotropy requires that $I \neq 0$ or $\frac{1}{2}$. Thus we have the significant immediate conclusion that the even-even 30-nsec ^{236m}Pu and 6-nsec ^{238m}Pu isomeric states are not the superfluid $I = 0$ lowest states at the second minimum. The uncertainties in the use of the above equations in the analysis of fragment anisotropies lies in the estimation of $G_\lambda(t)$ and $f(M)$. In two of the experiments (35, 37), the recoils were stopped in Pb, in the hope that the spin alignment could be preserved ($G_\lambda(t) \approx 1$) in the cubic lattice of metallic Pb. Recoiling into crystalline Pb does not assure that there will be no attenuation. Both instantaneous dislocations due to the stopping of the recoil atom and cumulative radiation damage due to the stopping of the fission fragments can give rise to attenuations. These problems are exacerbated by

Table 1 Fragment anisotropies for isomeric fission

Isomer	Half-life	$W(0°)/W(90°)$[a]	Reference
^{235m}Pu	30 nsec	1.1 ± 0.1	38
^{236m}Pu	30 nsec	0.70 ± 0.15	36
^{237m_1}Pu	114 nsec	0.90 ± 0.15	36
	45 nsec	0.58 ± 0.16	35
	100 nsec	0.4 ± 0.1	39
^{237m_2}Pu	1.1 μsec	1.41 ± 0.14	35
	1.1 μsec	1.9 ± 0.4	37[b]
^{238m}Pu	6 nsec	0.69 ± 0.09	35
^{239m}Pu	8 μsec	1.13 ± 0.04	40
^{240m}Pu	3.8 nsec	1.50 ± 0.8	36
^{241m}Cm	15 nsec	1.87 ± 0.40	36
	10 nsec	2.0 ± 0.4	35
^{243m}Cm	40 nsec	1.2 ± 0.4	36

[a] The anisotropies of Ref. 35 are $W(13°)/W(90°)$, rather than $W(0°)/W(90°)$.

[b] The anisotropy value of 1.9 given in this table differs from that reported in this reference, due to an additional correction for an A_4 term (J. Pedersen, private communication 1974).

Annu. Rev. Nucl. Sci. 1977.27:1-35. Downloaded from www.annualreviews.org
Access provided by 2409:4070:4701:c29b:fcdc:51af:e256:c850 on 09/30/22. For personal use only.

Annu. Rev. Nucl. Sci. 1977.27:1-35. Downloaded from www.annualreviews.org
Access provided by 2409:4070:4701:c29b:fcdc:51af:e256:c850 on 09/30/22. For personal use only.

the large quadrupole moments of shape isomers. The difficulty several workers (V. Metag, J. Pedersen, G. Sletten, private communication) have had in reproducing results suggests that the solid-state effects are not sufficiently well-understood at the present time to make reliable statements about the value of $G_\lambda(t)$. In the remaining experiment, the recoils were allowed to decay in flight in vacuum. Metag et al (41) conclude that 80% of the original alignment is preserved within the first 60 psec for recoil into vacuum. Most anisotropy measurements, however, have been performed for isomers with half-lives several orders of magnitude longer-lived than this. Comparison of the results of the different experiments in Table 1 indicates a lower value of the anisotropy for ^{237m}Pu when decaying in a vacuum compared to decaying in Pb, whereas similar anisotropies were observed for ^{241m}Cm. For spinless projectiles and targets, one would have $f(M = 0) = 1$ and $f(M \neq 0) = 0$ if the neutrons and γ rays did not carry off any angular momentum. The emission of neutrons and γ rays introduces a spread in $f(M)$. Since each emission carries off only a few units of angular momentum, and since the directions of emission are nearly isotropic and largely uncorrelated with one another, a statistical description should suffice for an approximate estimate of this distribution. The most serious shortcoming of this approximation may be contributions from stretched $E2$ transitions at the end of the γ cascade. This could be more important for α, $3n$ rather than α, $2n$ reactions, since the angular momentum input in the former is larger. Specht et al have assumed a Gaussian distribution of final M values, and estimated the dispersion of the distribution to be between 2 and 3. Hamamota & Ogle (42) have treated the γ cascade somewhat differently, and obtain considerably larger anisotropies for a given K and I combination. The calculations of Hien (43) give values qualitatively similar to those of Specht et al, but are sufficiently different to lead to different spin assignments for a given anisotropy. The spreading of the M distribution and the uncertainty in its width has a large effect on the expected anisotropies in all models. This is illustrated for the calculation of Specht et al in Figure 6. This uncertainty, together with the rather similar anisotropies expected for a number of different I and K_b combinations, means that unique spin assignments are not possible. In addition, one has uncertainties about the attenuation factors $G_\lambda(t)$, which have been assumed to be unity in all calculations. However, some valuable information not dependent on the details of the calculations or on the complete preservation of the alignment can be gleaned from anisotropy results.

We first discuss the interesting case of ^{237}Pu, where two different spontaneous-fission isomers have been discovered. The first attempt to gain information about the spins of the isomeric states was based on the relative populations of the two isomeric states in ^{237}Pu as a function of the angular momentum deposition in the reactions that produced them (44). The yield of the long-lived (1100-nsec) state relative to the short-lived (82-nsec) state increased with increasing angular momentum, showing that the long-lived isomer has a higher spin than the short-lived isomer. From Table 1 we see that the anisotropy for the short-lived state is less than unity, whereas that for the long-lived isomer is greater than unity. This difference implies that the upper (1100-ns) state decays primarily directly by fission rather than by a γ transition to the lower state followed by fission. It also demonstrates that the K value of the

second minimum state is not preserved during penetration through the barrier. From the absolute value of the anisotropies, the I value of the long-lived state would appear to be $\geqq \frac{5}{2}$, with K_b small compared to I. The I value of the short-lived state is poorly defined, with the K_b values having to be close to I for this state. If one requires the K_b value to be the same for the two states and uses the calculated anisotropies of Specht et al or of Hien [which include the dubious assumption that $G_\lambda(t) = 1$], this would limit the spin assignments to $I = \frac{11}{2}$ for the 1.1-μsec state and $I = \frac{5}{2}$ for the short-lived state, with $K_B = \frac{5}{2}$. This result is consistent with a hypothesis (32) that the upper and lower states correspond to the Nilsson orbitals $\frac{11}{2}+$ [615] and $\frac{5}{2}+$ [862]. These orbitals are close to the Fermi surface in most theoretical calculations (7, 8, 42, 45), as shown in Figure 7. They are not, however, consistent with the conclusions reached in an analysis of a g-factor measurement to be described later. If one makes the same requirement (that K_B be the same for both states) and uses the calculated anisotropies of Hamamoto & Ogle, assignments of $I = \frac{7}{2}$ and $\frac{3}{2}$ with $K_B = \frac{3}{2}$ would be indicated.

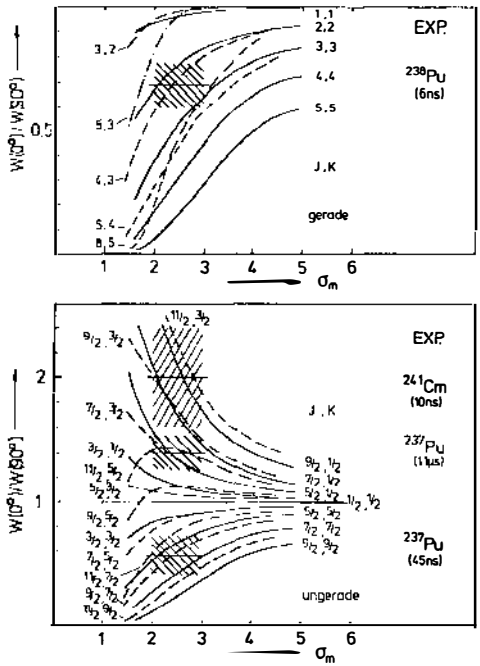

Figure 6 Calculated anisotropies $W(0°)/W(90°)$ as a function of the Gaussian width σ_M of the substate occupation number distribution function $f(M)$ for all combinations of I and K (up to $\frac{11}{2}$), for even (*a*) and odd (*b*) nuclei. The shaded areas represent the experimental anisotropies of the four isomers with their experimental errors and the uncertainty in the width σ_M. From Specht et al (35).

Annu. Rev. Nucl. Sci. 1977.27:1-35. Downloaded from www.annualreviews.org
Access provided by 2409:4070:4701:c29b:fcdc:51af:e256:c850 on 09/30/22. For personal use only.

The anisotropy for ^{241m}Cm requires that $I \geqq \frac{7}{2}$ with K_B small. The small anisotropy for the ^{243m}Cm isomer does not allow anything quantitative to be concluded.

NUCLEAR G-FACTORS Further information about the properties of single-particle states of shape-isomeric nuclei can be obtained if the nuclear g-factor can be measured. Although such measurements are very difficult, preliminary results have been obtained for both the 1.1- and 0.1-μsec isomers of ^{237m}Pu. The technique used is to measure the time-dependent angular distribution of delayed-fission fragments when an external magnetic field is applied perpendicular to the plane of the detectors and target. The time-dependent angular distribution is obtained from an extension of Equation 1,

$$W^{I}_{K_b}(\theta, t) = \sum_{\lambda} A_\lambda G_\lambda(t) P_\lambda \cos(\theta - \omega_L t), \qquad 3.$$

with the Larmor precession frequency

$$\omega_L = -g B_{\text{eff}} \mu_N / \hbar. \qquad 4.$$

If only the $\lambda = 0$ and $\lambda = 2$ terms are significant, the difference in counts between one detector at $+\theta$ and another at $-\theta$ with respect to the beam has an exponentially decaying time dependence modulated by twice the Larmor precession frequency. If, in addition to being placed at $\pm\theta$ with respect to the beam, the detectors are also placed at 90° with respect to each other, the difference in counts between the detectors divided by the sum of the counts gives a simple sinusoidal time dependence. A

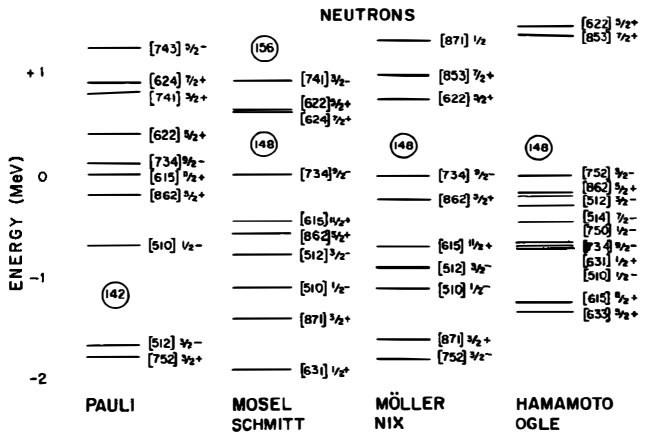

Figure 7 Neutron single-particle levels at the deformation corresponding to the second minimum. This diagram has been constructed from calculations reported by Pauli (7), Mosel & Schmitt (45), Möller & Nix (8), and Hamamoto & Ogle (42). Occasionally, significant mixing between orbitals occurs and the orbital labels are no longer very meaningful, for example the $[633]\frac{5}{2}^+$ and $[862]\frac{5}{2}^+$ orbitals, which are strongly mixed at this deformation in the calculation of Hamamoto & Ogle.

Annu. Rev. Nucl. Sci. 1977.27:1-35. Downloaded from www.annualreviews.org
Access provided by 2409:4070:4701:c29b:fcdc:51af:e256:c850 on 09/30/22. For personal use only.

knowledge of the sign of the effective magnetic field B_{eff} (including both external and internal components) together with the sign of A_2, which can be obtained from an independent measurement of the time-integrated anisotropy $W(0°)/W(90°)$, enables one to obtain the sign of g from the phase of the oscillations. The g-factors for both the 1.1-μsec (37) and 0.1-μsec (39) isomers have been determined to be positive.

The absolute magnitude of g depends on a knowledge of $B_{eff} = \beta B_{ext}$, where β is the paramagnetic correction factor. This correction factor depends on the ionic state of the recoil Pu ion in the stopping Pb environment and, with certain assumptions, can be calculated for an assumed ionic charge. As defined, β has contributions from both a temperature-dependent part from the partial polarization of the $5f$ electrons and a temperature-independent part from the direct effect of the external field. The relative magnitudes of the two terms are different for each ionic state, so that a measurement of the temperature dependence of the precession frequency in principle enables one to determine β experimentally. In the experiment of Kalish et al, a measurement of the temperature dependence was used to decide between calculated values of β for 3+ and 4+ ionization states, with the results indicating the 4+ ionization state was involved. With this determination, g values of 0.14 ± 0.02 and 0.44 ± 0.05 were obtained for the 1.1- and 0.1-μsec isomeric states, respectively. The errors indicated do not include uncertainties in the β value, which might be as large as 30%.

In comparing the experimental values with theory, it is important to note that the isomeric state is presumed to have $K = I$ while precessing in the magnetic field, even if, during the leakage through the barrier, the effective value K_B is different than that of K. The theoretical estimate for the g-factor for a single-particle state described by the quantum numbers K and I moving in an axially symmetric potential can be written as

$$g = \left(1 - \frac{K^2}{I(I+1)}\right) g_R + \frac{K^2}{I(I+1)} g_\Omega, \quad K \neq \tfrac{1}{2}, \qquad 5.$$

with

$$\Omega g_\Omega = g_l \langle l_3 \rangle + g_S \langle S_3 \rangle. \qquad 6.$$

Here g_R represents the magnetic moment due to the collective flow of protons and neutrons, whereas g_Ω results from the unpaired particle. The terms g_l and g_S arise from the orbital and intrinsic spin contributions to the g-factor, with l_3 and S_3 the components of the orbital and intrinsic spin angular momenta along the nuclear symmetry axis. These components can be calculated from the wave functions for single-particle states in the deformed potential. Orbitals with the Nilsson quantum numbers $\Sigma = \Omega - \Lambda = +\frac{1}{2}$, corresponding to parallel coupling of the orbital and spin angular momenta, have S_3 positive, and orbitals with $\Sigma = \Omega - \Lambda = -\frac{1}{2}$ have S_3 negative. The absolute values of S_3 can be reduced significantly from $\frac{1}{2}$ (reductions of up to 50% are calculated and observed for rare-earth nuclei (46) since the spin-orbit part of the potential can result in significant admixtures of components with the opposite sign. This has the consequence that the expected g_Ω values for different Ω values can overlap. Additional uncertainties arise from inadequate knowledge about

Annu. Rev. Nucl. Sci. 1977.27:1-35. Downloaded from www.annualreviews.org
Access provided by 2409:4070:4701:c29b:fcdc:51af:e256:c850 on 09/30/22. For personal use only.

g_R, g_l, and g_S. For deformed rare-earth nuclei, empirical effective values of $g_R = 0.35 \pm 0.4$, $g_l^{eff}(n) = -0.03 \pm 0.04$, $g_l^{eff}(p) = 1.07 \pm 0.04$, $g_S^{eff}(n) = -2.4 \pm 0.6$, $g_S^{eff}(p) = 3.7 \pm 0.6$ have been deduced (47, 48). These g_S values are significantly reduced (by a factor of about ~ 0.65) from the free-particle values.

The reported positive sign of g for both the 1.1- and 0.1-μsec ^{237m}Pu isomeric state implies that the relevant Nilsson orbitals have quantum numbers $\Omega - \Lambda = -\frac{1}{2}$. This is in disagreement with the earlier suggestion that these states correspond to the $\frac{11}{2}+[615]$ and $\frac{5}{2}+[862]$ orbitals. Hamamoto & Ogle (42) have calculated g values for several orbitals close to the Fermi surface for the second minimum. These results are given in Table 2.

Some readjustments of their standard parameters are required to reproduce the experimental $g = 0.14$ value for the 1.1-μsec state, with $\frac{5}{2}+[633+862]$, $\frac{7}{2}-[514]$ and $\frac{3}{2}-[752]$ orbitals being possible candidates. The $\frac{3}{2}-[512]$ and $\frac{7}{2}-[514]$ orbitals could be candidates for the 0.1-μsec state with $g = 0.44$. These suggestions must be considered very tentative at this time, in view of the preliminary nature of the experimental results and the fact that the theoretical calculation used a spin-orbit strength stronger than that indicated by the experimental level ordering at smaller deformations.

MOMENTS OF INERTIA As discussed later, the lowest-lying levels of even-even nuclei are rotational in character. If the energy spacings between these levels can be determined for a shape-isomeric nucleus, the moment of inertia can be deduced. The transitions between these low-lying levels are highly converted, yielding low-energy

Table 2 Estimated g-factors for four states in the region of the second minimum for ^{237}Pu[a]

	Calculated				
I	Orbital		Parameters	g_{min}	g^{max}
$\frac{7}{2}$	$\frac{7}{2}^-$	514	standard	0.22	0.41
$\frac{5}{2}$	$\frac{5}{2}^+$	(633)	standard	−0.04	0.05
			$\eta_2 = 0.70$	0.12	0.24
			$\eta_4 = 0.08$	0.05	0.13
$\frac{3}{2}$	$\frac{3}{2}^-$	512	standard	0.42	0.70
$\frac{3}{2}$	$\frac{3}{2}^-$	752	standard	0.00	0.10
	Experimental				
	$g_{exp}(1.1\ \mu sec) = 0.14 \pm 0.05$[b]				
	$g_{exp}(0.1\ \mu sec) = 0.44 \pm 0.14$				

[a] The values were calculated (42) for a variation of the g_R, g_l, and g_S factors given by $0.25 \leq g_R \leq 0.40$, $-0.08 \leq g_l \leq -0.04$, and $0.65 \leq (g_S)_{eff}/(g_S)_{free} \leq 1.0$.

[b] Experimental values from Kalish et al (37) and Shackleton et al (39). The errors are our estimates, which include the uncertainties in β, as well as the statistical errors in determining the Larmor frequencies.

Annu. Rev. Nucl. Sci. 1977.27:1-35. Downloaded from www.annualreviews.org
Access provided by 2409:4070:4701:c29b:fcdc:51af:e256:c850 on 09/30/22. For personal use only.

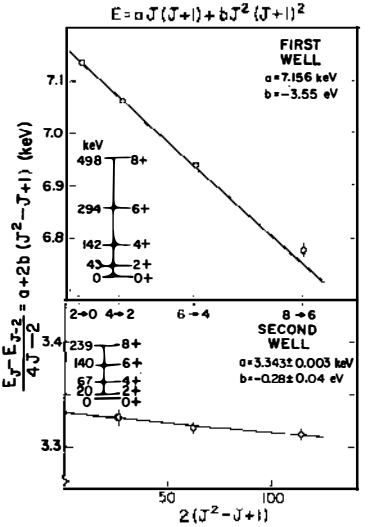

Figure 8 Fit of the transition energies to the energy expression $E = aJ(J+1) + bJ^2(J+1)^2$ (*a*) for the ground-state band of the first well and (*b*) for the isomeric-state band of the second well. The intercept gives the rotational constant *a* and the slope the non-adiabaticity parameter *b*. (After Specht and co-workers (49) and including corrections for the high–ionic charge states (see footnote 2).

conversion electrons. The observation of these electrons is very difficult, as the feeding of the isomer rotational band is usually at least 10^4 times smaller than that of the ground-state band, and there are also many other sources of low-energy electrons in the experiments where the isomers are produced. In spite of these difficulties, conversion electron groups from several transitions in each of two shape-isomeric nuclei have been observed. Specht et al (49) have studied ^{240m}Pu produced in an (α, 2*n*) reaction, while Borggreen et al (50) have studied ^{236m}U produced in a (*d*, *p*) reaction. The identification of electrons associated with the de-excitation of the rotational band built on the shape-isomeric state was performed using a delayed coincidence between the electrons and the fission fragments from the subsequent decay of the isomer. The level scheme deduced for ^{240}Pu is shown in the inset of Figure 8. The value of $\hbar^2/2\mathscr{I}$ obtained for ^{240}Pu is 3.343 ± 0.003 keV,[2] and for ^{236}U is 3.36 ± 0.01 keV. These values are less than half the values exhibited by the ground-state rotational bands, and provide fairly direct evidence that the shape isomer has a distortion qualitatively different from that of the ground state.

The moments of inertia depend not only on the shape (deformation) of the

[2] This value is slightly different than the value given in the original paper, due to a correction for the high ionic charges of the atoms. The new values are 46.72 ± 0.09 keV, 73.12 ± 0.12 keV, and 99.35 ± 0.13 keV for the $4+ \rightarrow 2+$, $6+ \rightarrow 4+$, and $8+ \rightarrow 6+$ transitions (H. J. Specht, private communication).

Annu. Rev. Nucl. Sci. 1977.27:1-35. Downloaded from www.annualreviews.org
Access provided by 2409:4070:4701:c29b:fcdc:51af:e256:c850 on 09/30/22. For personal use only.

Annu. Rev. Nucl. Sci. 1977.27:1-35. Downloaded from www.annualreviews.org
Access provided by 2409:4070:4701:c29b:fcdc:51af:e256:c850 on 09/30/22. For personal use only.

nucleus, but also on the nature of the mass motion. The moments of inertia of ground-state deformed nuclei are considerably reduced from rigid-body moments. This reduction can largely be reproduced in microscopic calculations using the cranking model and including pairing interactions (51). Several such calculations have been extended to include deformations corresponding to the shape-isomeric state (52–56). Both the calculated and experimental values of the ratio of the moment of inertia of the shape-isomeric state to that of the ground state is larger than that for a rigid rotator, reflecting the fact that the true moment of inertia more nearly approaches the rigid-body limit at large deformations. This result is illustrated in Figure 9. Most calculations tend to underestimate slightly ($\sim 15\%$) the moments of inertia at the ground state. The discrepancy is reduced in the calculations of Hamamoto (56), which include an additional term arising from the rotational motion on the pairing correlation. This calculation, however, overestimates the moment or inertia of the shape isomer. All of the calculations are somewhat sensitive to the assumed dependence of the pairing-strength parameter G on deformation. Calculations with both a constant pairing strength (G = const.) and with a pairing strength proportional to the surface area S ($G \propto S$), have been performed. It is unlikely (57) that the dependence of the pairing strength on surface area S is as strong as $G \propto S$.

QUADRUPOLE MOMENTS The quadrupole moment of a nuclear state also provides information on the nuclear deformation. In fact, the relation between the static quadrupole moment and the shape is less model-dependent than is the relation between the moment of inertia and the shape. Two rather different experimental approaches (58, 59) have been used recently to measure or deduce the lifetimes for rotational transitions feeding a fission isomeric state. If the transitions are primarily $E2$ in character, it is possible to deduce the quadrupole moment from the observed lifetimes. Since the expected lifetimes are sub-nanosecond, direct electronic timing experiments are not feasible.

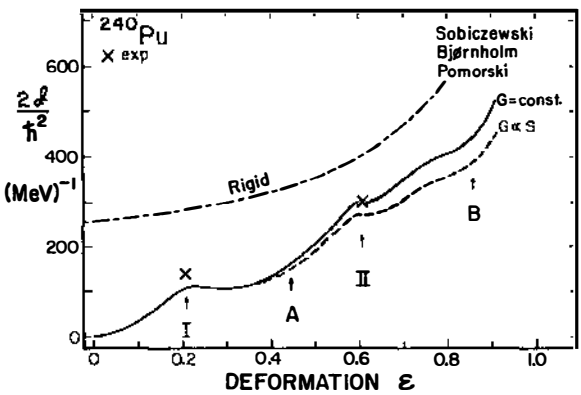

Figure 9 Comparison of theoretical and experimental values of the moment of inertia as a function of deformation. After Sobiczewski et al (54).

An ingenious "charge plunger" technique, capable of working in the same approximate time range as the Doppler-shift plunger technique, has been developed at Heidelberg (58). It is based on the fact that the rotational transitions in highly deformed nuclei are largely converted, that is, decay by internal conversion. The fast Auger cascades following such transitions lead to ionic charge states typically an order of magnitude larger than the equilibrium charge states (1^+–2^+) at the recoil velocities present. In the experiment, the recoiling ions are passed through a charge-resetting foil placed at various distances from the target. If the rotational de-excitation cascade is completed prior to arriving at the charge-resetting foil, the emerging ions will retain the small equilibrium charged attained for the rest of their flight, whereas if a converted transition occurs after reaching the foil, there will be a large increase in the ionic charge. The relative numbers of ions with low and high ionic charges can be determined by deflecting the ions in a magnetic field and recording the subsequent spontaneous fission in track detectors placed as recoil collectors. The time scale of the rotational de-excitation cascade can be determined by measuring the intensity ratio of the high-charge and low-charge components as a function of the distance between the target and the charge-resetting foil.

This technique has been applied to a study of the rotational band feeding the 8-μsec isomer of ^{239}Pu produced by a $\alpha, 3n$ reaction. In this first experiment an odd-A nucleus was chosen because of yield and half-life considerations. For an odd-A nucleus, however, the lifetimes are sensitive to the K value of the band as well as to the quadrupole moment. For small K- values, the transitions become very low in energy and are slowed down. Without a knowledge of the K value it is not possible to determine the quadrupole moment uniquely. Comparison of the observed decay curve (corrected for a long-lived component) with rotational-model calculations for various K values and an assumed quadrupole moment $Q_0 = 36.0$ b is shown in Figure 10. It is claimed that for K values of $\leq\frac{3}{2}$, the calculated decay curves are

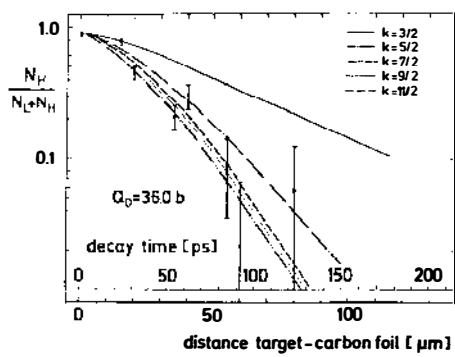

Figure 10 Fraction of highly charged recoil ions as a function of distance (or flight time) between target and charge-resetting foil. Corrections for a longer-lived 12-nsec component have been made. The theoretical curves represent cascade calculations for different K values of the rotational band and a quadrupole moment Q_0 of 36 b. From Habs et al (58).

Annu. Rev. Nucl. Sci. 1977.27:1-35. Downloaded from www.annualreviews.org
Access provided by 2409:4070:4701:c29b:fcdc:51af:e256:c850 on 09/30/22. For personal use only.

inconsistent with the experimental data. For K values $K \geqq \frac{5}{2}$, the quadrupole moment is determined to be $Q_0 = (36.0 \pm 4.4)$ b.

A rather different approach has been used by Metag & Sletten (59) at Copenhagen to deduce the rotational-state lifetimes. The branching ratios for spontaneous fission and electromagnetic decay of the rotational states are inferred from the angular distribution of delayed fragments. The lowest 0+ state decays isotropically, but the higher states contribute increasingly to an anisotropic decay pattern. The expected anisotropy associated with decay from each rotational state is calculated in a manner similar to that described previously. The relative population of the different rotational levels and their partial spontaneous-fission lifetimes must be estimated in order to deduce the quadrupole moment from the anisotropy. The result, however, is not sensitive to side-feeding times into the rotational band, as is the previous method discussed. The method requires an isomer with a very short half-life so that the rotational de-excitation and fission lifetimes will be comparable. The 37-psec isomer of ^{236}Pu has been investigated. The value of the quadrupole moment deduced from the anisotropy of 1.48 ± 0.15 is 37^{+14}_{-8} b.

These values of the quadrupole moment are in very good agreement with theoretical estimates (18, 55, 60, 61). If the shape of the nucleus in the isomeric state is approximated by a prolate spheroid, a quadrupole moment of 36 ± 4.4 b corresponds to an axis ratio of (1.95 ± 0.1) for a radius parameter of $r_0 = 1.20$ fm (58).

DECAY PROPERTIES

Half-lives and Barrier Penetrabilities

The half-lives of known spontaneously fissioning isomers span the range from 10^{-11} to 10^{-2} sec. The lower end of the range is determined by the limitations of current experimental techniques. The development of a projection method (62) for determining half-lives as short as 10^{-11} sec is in fact a remarkable achievement,

Table 3 New isomer half-life data since the compilation of Britt (67)

Nuclide	Half-life	Reference
^{236m}U	116 ± 7 nsec	64
^{236m}Pu	37 ± 4 psec	63, V. Metag, private communication
^{238m}Pu	0.6 ± 0.2 nsec	63, 65
^{239m_2}Pu	12 ± 7 nsec	58
^{242m}Pu	3.5 ± 0.6 nsec	63
^{244m}Pu	380 ± 80 psec	63
^{240m_1}Cm	55 ± 12 nsec	66
^{240m_2}Cm	10 ± 3 psec	66
^{242m}Cm	40 ± 15 psec	66
^{244m}Cm	$\leqq 5$ psec	66

Annu. Rev. Nucl. Sci. 1977.27:1-35. Downloaded from www.annualreviews.org
Access provided by 2409:4070:4701:c29b:fcdc:51af:e256:c850 on 09/30/22. For personal use only.

particularly in consideration of the low yields of delayed fission relative to prompt fission encountered (10^{-5}–10^{-6}). The new results (63) obtained with this technique, as well as other new half-life information (64–66) obtained since the compilation of Britt (67), are given in Table 3. A plot of isomeric half-lives as a function of neutron number for different elements is given in Figure 11. A few even-even isomers in Pu and Cm, believed to be two-quasiparticle excitations, have been omitted from this plot. The paucity of information on spontaneous-fission isomers of Np and U is attributed to predominant decay by γ decay rather than by fission decay. The sensitivity of detection for γ decay is much poorer than for fission decay, and γ radiation is less characteristic of shape isomerism. The observed dependence on neutron number makes it unlikely that isomers longer-lived than 14-ms ^{242}Am will be found, with the possible exception of odd-odd Np isomers, which might have very weak fission decay modes. A number of systematic features are revealed in

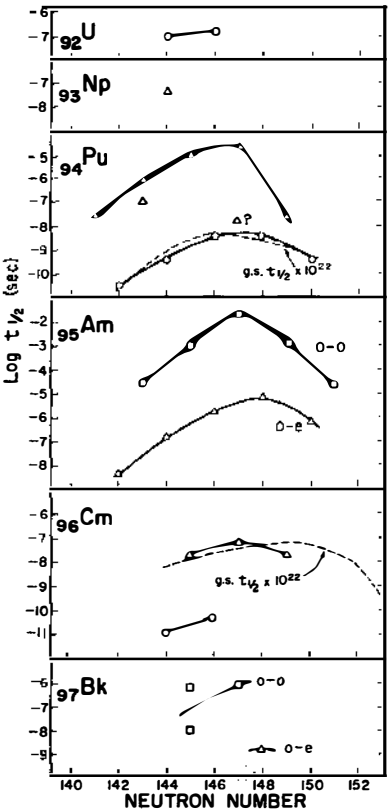

Figure 11 Spontaneously fissioning isomer half-lives as a function of neutron number. Circles, triangles, and squares represent values for even-even, odd-A, and odd-odd nuclei, respectively. Updated version of figure from (32).

Annu. Rev. Nucl. Sci. 1977.27:1-35. Downloaded from www.annualreviews.org
Access provided by 2409:4070:4701:c29b:fcdc:51af:e256:c850 on 09/30/22. For personal use only.

Figure 11. The first of these is the maximum in the half-life at $N = 146$. This is qualitatively consistent with the variation of the calculated neutron-shell correction at the second minimum with neutron number, and corresponds approximately with gaps in the single-particle spectra calculated by various authors (see Figure 7).

An attempt to understand the effect of the interplay between the shell corrections at the second minimum and at the outer barrier on the neutron-number dependence of the half-lives has been given elsewhere (32). The variation in isomer half-lives with neutron number is surprisingly similar to that exhibited by the ground-state half-lives, although there is an upward shift in the neutron number corresponding to the longest half-lives as one goes from the isomeric states to the ground states. To the extent that the similarity arises from shell effects, one would expect it to be primarily due to effects at the outer barrier that are common to both ground and isomer decays.

A plot of the isomer half-lives versus proton number, rather than neutron number, yields points that fall on straight lines for a given neutron number (30). Three lines are obtained for a given neutron number, corresponding to even-even, odd-even, and odd-odd nuclei. The linear falloff of the logarithm of the half-life with increasing proton number is qualitatively consistent with the decrease of the liquid-drop part of the height of the outer barrier with increasing Z^2/A. The dependence of the shell correction on proton number is apparently considerably weaker than that for neutrons and does not appear in the form of a further modulation of the dependence of the half-lives on proton number. This is consistent with theoretical calculations that indicate that spontaneous-fission isomerism results primarily from a neutron-shell effect and not a proton-shell effect. This weakens the argument that fission isomers simply reflect the particular degeneracies of the single-particle states for a deformed potential corresponding to a shape whose semi-axes are in the ratio of 2 : 1.

Another feature revealed in Figure 11 is the large retardation of the half-lives for odd-A and odd-odd nuclei compared to even-even nuclei. This retardation also appears to be somewhat more regular than that exhibited by ground-state half-lives. Some tendency for smaller fluctuations in the isomer half-lives may arise from the fact that an alternate decay path is available, i.e. γ decay back to the first minimum. Thus very large retardations may not appear if the partial half-life for decay through the outer barrier becomes long compared to that for decay through the inner barrier. Returning to the average retardation of the decay for odd-A and odd-odd nuclei, two possible origins of this retardation can be identified by consideration of the expression for penetration through an idealized parabolic barrier. The penetration p is given by $p = \exp\left[-2\pi(E_B - E_{II})/\hbar\omega_B\right]$. The presence of unpaired particles may increase the height of the barrier that must be penetrated, $E_B - E_{II}$, by an amount sometimes designated as the "specialization" energy (68). Unpaired particles are also expected to increase the inertial mass and hence decrease the parameter $\hbar\omega_B$. In a previous examination (32) of this problem, we have determined the approximate magnitudes of each of these two effects that would be required to account for the observations if the other effect were absent. Specialization energies of 0.8 and 1.7 MeV for odd-A and odd-odd nuclei, respectively, would be required in the absence of any effect on $\hbar\omega_B$. Conversely, 25% and 45% decreases in $\hbar\omega$ would be required in the

Annu. Rev. Nucl. Sci. 1977.27:1-35. Downloaded from www.annualreviews.org
Access provided by 2409:4070:4701:c29b:fcdc:51af:e256:c850 on 09/30/22. For personal use only.

absence of specialization-energy effects. Metag (30) has performed a more quantitative examination of this problem by performing a 5-parameter least-squares fit to the half-lives of 33 isomers. In this fit, an odd-even effect on both the barrier height and on $\hbar\omega_B$ was allowed. For odd-mass nuclei, a specialization energy of 0.3 MeV and a decrease in $\hbar\omega_B$ of 16% was found. This decrease in $\hbar\omega_B$ of 16% corresponds to an increase in the inertial mass parameter of 30% if the curvature of the barrier is not changed by the addition of the unpaired particle. This result is in good agreement with theoretical estimates of the increase of the inertial mass parameter due to blocking effects of the odd particle (69–71).

The semi-empirical formula used by Metag to fit the half-lives is given by

$$t_{1/2}^{S.F.} = (\ln 2)(4 \times 10^{-21})\left\{1+\exp\frac{2\pi}{\hbar\omega}[ax+b(N-N_0)^2+d+S)]\right\},$$

with

$$\hbar\omega = \hbar\omega_0 \begin{cases} 1/\delta & \text{odd-odd} \\ 1 & \text{odd-even} \\ \delta & \text{even-even} \end{cases} \quad \text{and } S = \begin{matrix} 2S_0 \\ S_0 \\ 0 \end{matrix} \begin{cases} \text{odd-odd} \\ \text{odd-even,} \\ \text{even-even} \end{cases}$$

and where the fissility parameter x was assumed to be

$$x = \frac{Z^2/A}{2(a_S/a_c)\{1-[\kappa(N-Z)^2/A^2]\}},$$

with $\kappa = 1.87$, $a_S = 17.64$ MeV, and $a_c = 0.72$ MeV. Shell effects are introduced through the dependence on $(N-N_0)$, where the magic number N_0 was found to be 146. (Theoretical calculations give magic numbers of 142 or 148 as shown in Figure 7.) An attempt to include proton-shell effects showed that they were an order of magnitude smaller. A least-squares fit gave the following values of the parameters:

$$\frac{a}{\hbar\omega_0} = -49.4 \pm 5.2,$$

$$\frac{b}{\hbar\omega_0} = -(3.9 \pm 0.4) \times 10^{-2},$$

$$\frac{d}{\hbar\omega_0} = 46.0 \pm 4.4,$$

$$\frac{S_0}{\hbar\omega_0} = 0.43 \pm 0.26,$$

$$\delta = 1.16 \pm 0.08.$$

A comparison of the experimental half-lives with the calculated values from the five-parameter fit is shown in Figure 12. The success of this parameterization suggests that the curves in this figure will have fairly good predictive power for isomers that have yet to be identified.

There have been two recent attempts to calculate both ground- and isomer-state

Annu. Rev. Nucl. Sci. 1977.27:1-35. Downloaded from www.annualreviews.org
Access provided by 2409:4070:4701:c29b:fcdc:51af:e256:c850 on 09/30/22. For personal use only.

lifetimes from potential energy surfaces obtained by the shell-correction method and microscopic inertial parameters calculated with the cranking model (72–74). The adiabatic approximation is made and the penetrability is calculated using the WKB approximation. The mean lifetime for spontaneous fission may be written as

$$\tau = \frac{2\pi}{\omega_f} \exp(2S/\hbar) \qquad 7.$$

where $\omega_f/2\pi$ is the frequency of barrier assaults and the action integral S is given by

$$S = \int_{r_1}^{r_2} [2B(r)(V_{(r)} - E_{vib})]^{1/2}\, dr. \qquad 8.$$

The action integral has to be calculated along the trajectory of least action, determined by $\delta S = 0$. This leads to a multidimensional problem for which both the potential energies and the inertial parameters have to be calculated as a function of all the relevant shape degrees of freedom. Ledergerber & Pauli (72) have pointed out some interesting features of this problem. As a practical matter, they have found the least-action path by trial. Although there is some correlation of the inertial parameter

$$T_{1/2}^{s.f.} = \ln 2 \cdot 4 \cdot 10^{-21} \left(1 + \exp\left(\frac{2\pi}{\hbar\omega}(aX + b(N-N_0)^2 + d + S)\right)\right) \qquad \hbar\omega = \hbar\omega_0 \cdot \begin{cases} 1/5 \\ 1.0 \\ 5 \end{cases} \qquad S = \begin{cases} 2S_0 & \text{odd-odd} \\ S_0 & \text{odd-even} \\ 0 & \text{even-even} \end{cases}$$

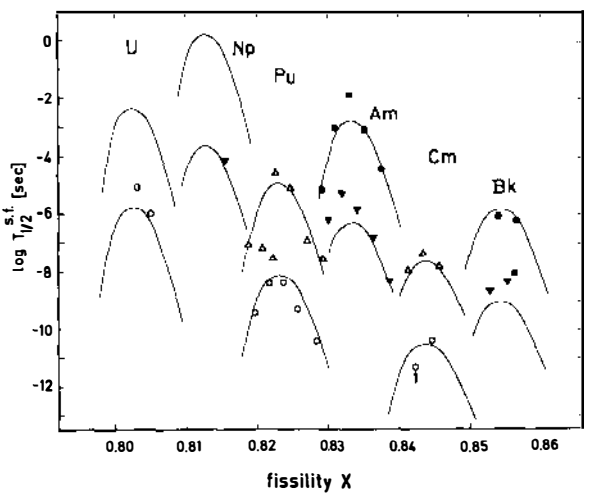

Figure 12 Half-lives for spontaneous fission from shape-isomeric states in U, Np, Pu, Am, Cm, and Bk isotopes as a function of the fissility parameter x. Open circles refer to isomers in even-even nuclei, triangles to isomers in odd-mass nuclei, and closed circles to isomers in odd-odd nuclei. Solid curves represent half-lives calculated with a 5-parameter semi-empirical formula whose parameters were determined by a least-squares fit to the experimental data and are given in the text. After Metag (30).

Annu. Rev. Nucl. Sci. 1977.27:1-35. Downloaded from www.annualreviews.org
Access provided by 2409:4070:4701:c29b:fcdc:51af:e256:c850 on 09/30/22. For personal use only.

Annu. Rev. Nucl. Sci. 1977.27:1-35. Downloaded from www.annualreviews.org
Access provided by 2409:4070:4701:c29b:fcdc:51af:e256:c850 on 09/30/22. For personal use only.

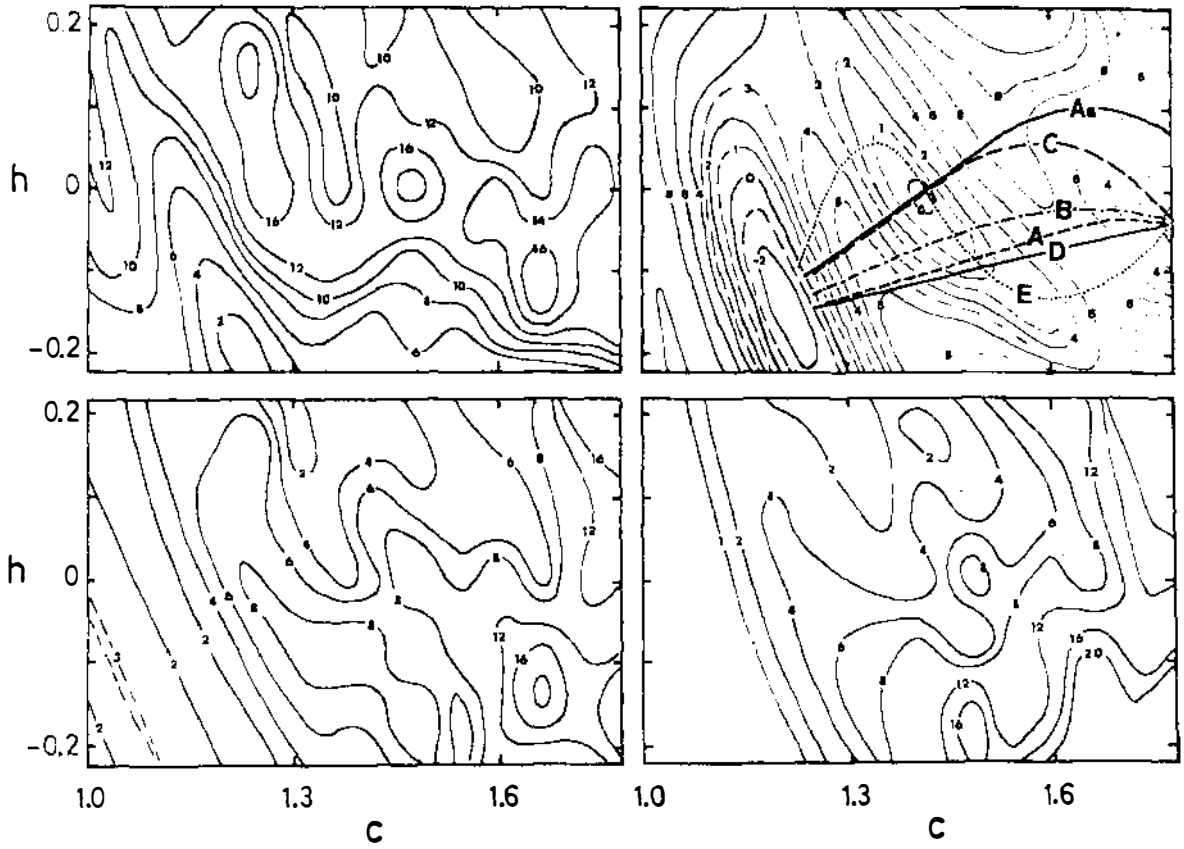

Figure 13 The deformation energy W (*upper right*) and the mass parameters B_{cc} (*upper left*), B_{ch} (*lower left*), and B_{hh} (*lower right*) of ^{240}Pu versus the two symmetric deformations c and $h(x = 0)$ are shown as contour plots. The mass parameters are given in units of 100 $\hbar \cdot \mathrm{MeV}^{-1}$; the energy is in MeV. In the plot of the deformation energy, some fission trajectories, leading from the ground-state well to the exit region, are shown by thicker lines. The values of the corresponding action integrals are: $S = 60.25\ \hbar$ (A), $60.4\ \hbar$ (B), $60.3\ \hbar$ (C), $60.9\ \hbar$ (D), $66.1\ \hbar$ (E), $70\ \hbar$ (As). The

Annu. Rev. Nucl. Sci. 1977.27:1-35. Downloaded from www.annualreviews.org
Access provided by 2409:4070:4701:c29b:fcdc:51af:e256:c850 on 09/30/22. For personal use only.

with the shell-correction energy, the least-action path does not follow the apparent path of steepest descent. This is illustrated in Figure 13. One must remember, however, when examining the potential energy surface, that the shape of such a surface is dependent on the choice of parameters against which it is plotted. Certain features such as local maxima, local minima, and saddle points are invariant under coordinate transformations (75). Several paths are shown superimposed on the potential energy surface in the upper right-hand corner of this figure. The path *E*, which is closest to the path of steepest descent that would go through the saddle between the ground- and shape-isomer minima, has a considerably larger integral (less favorable penetrability) than the path *A*, which tunnels through a region where the potential energy is higher. A consequence of this result is the difficulty of defining a proper fission barrier. A "dynamic" barrier, which, following Ledergerber & Pauli, we define as the maximum in the potential energy along the path of least action, may be an MeV or so larger than the static barrier, defined as the saddle point in the deformation energy landscape. Thus the effective barrier height may depend on the collective kinetic energy with which the barrier is approached.

Another important result of these investigations is the decrease in the action integral obtained when reflection-asymmetric degrees of freedom are taken into account for deformations larger than the second minimum. For ^{240}Pu, the lowest action for a symmetric trajectory is 60.25 $\hbar$, whereas for an asymmetric trajectory it can be lowered to 52.8 $\hbar$, leading to a reduction in the calculated lifetime of a much needed factor of more than 10^7. Ledergerber & Pauli (72) have also noted a correlation between a parameter characterizing the asymmetry of the nuclear shape at the "dynamic" outer barrier defined above and the experimental mass asymmetry for nuclei from uranium to fermium.

Branching Ratios

The most easily detected and presumably the most important mode of decay for presently known shape isomers in the actinide region is spontaneous fission. An alternative mode of decay is by γ emission to lower-lying states in the first minimum. The relative probability for these processes depends both on the penetrabilities of the inner and outer barriers and on the hindrance of the γ decay process relative to fission (76). There are both theoretical and empirical indications that the inner barriers should become more penetrable relative to the outer barriers for the lower-*Z* elements. Theoretical calculations show that the inner barrier is the higher of the two barriers for plutonium and higher-*Z* actinides and that the outer barrier is the higher for the lower-*Z* actinides (27, 77). The systematic trend is in part the consequence of the inward shift in deformation of the liquid-drop part of the fission barrier as *Z* decreases. More difficult to estimate theoretically are the effects of the barrier width and inertial paramaters on the penetrability. The calculations of Ledergerber & Pauli (72) (see Table 1 of this reference) show that the inner barrier can be considerably more penetrable than the outer barrier even when the inner barrier is the higher of the two. In terms of a simple one-dimensional parabolic barrier, this would correspond to barrier curvature energies $\hbar\omega_A > \hbar\omega_B$. Experimental determinations (14) of the barrier heights E_A and E_B show $E_A < E_B$ for Pu and higher-*Z* even-even

actinides, comparable to values of E_A and E_B for uranium, and $E_A < E_B$ for thorium isotopes. The analysis of the direct-reaction fission probabilities show that the $\hbar\omega$ values determining the penetrability and reflection near the top of the barrier are characterized by $\hbar\omega_A > \hbar\omega_B$ for almost all even-even actinide nuclei. These results are illustrated in Figure 14.

Motivated by these results, together with the indications from fission-yield systematics that there might be a sizable non-fission decay branch, Russo et al (13) searched for a γ decay branch for the ^{238}U shape isomer. The γ decay mode is much more difficult to observe experimentally than the fission decay mode because of high backgrounds of delayed γ rays from fission fragments and because of lower absolute detection efficiencies for γ rays. Such measurements are therefore only possible if there is a sizable branching ratio for γ decay relative to fission. Two γ-ray lines were found with half-lives in agreement with that observed for the fission branch. These γ rays have energies of 1.879 and 2.514 MeV, giving an energy difference consistent with the previously known difference between the lowest 1− and 2+ levels of ^{238}U. These lines have therefore been attributed to decays leading to these states, as indicated by the decay scheme in Figure 15. The sum of the yields of these two states is more than 20 times larger than the yield for fission decay of the isomer. An estimate of the unobserved yield to higher states would increase this ratio by about a factor of 2. These results, together with a model-dependent estimate (78) of the hindrance of γ decay relative to fission, lead to a ratio of the penetrability of the inner barrier P_A to the outer barrier P_B of 4×10^7. Taking $E_A = 5.90$ MeV and

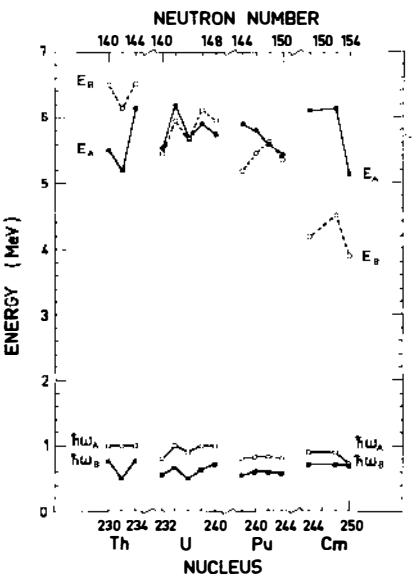

Figure 14 Fission-barrier parameters determined from the analysis of fission probabilities. From Back et al (14).

Annu. Rev. Nucl. Sci. 1977.27:1-35. Downloaded from www.annualreviews.org
Access provided by 2409:4070:4701:c29b:fcdc:51af:e256:c850 on 09/30/22. For personal use only.

$E_B = 6.17$ (14), and assuming parabolic barriers leads to $\hbar\omega_A = 1.18$ MeV and $\hbar\omega_B = 0.63$. The predominance of γ decay over fission decay for ^{238m}U is more a consequence of the "thinner" inner barrier, reflected by $\hbar\omega_A > \hbar\omega_B$, than of the slightly lower value of E_A relative to E_B. The absolute values of $\hbar\omega_A$ and $\hbar\omega_B$ deduced are somewhat larger than the values deduced from direct-reaction fission probability data (14), perhaps reflecting the fact that the latter determination is only sensitive to the curvature near the top of the barrier, while decay of the shape isomer involves penetration 3 MeV below the top of the barrier.

There is a preliminary report from Heidelberg (79) on the observation of a γ-ray line at 2.215 MeV with a half-life of 104 ± 19 nsec produced in the $^{235}U(d, p)$ reaction. This half-life is in good agreement with the value 116 ± 7 nsec observed for delayed fission of ^{236m}U (64). If this transition populates the first rotational level of the ground state, the isomer excitation energy is 2.26 MeV. The population of this isomer

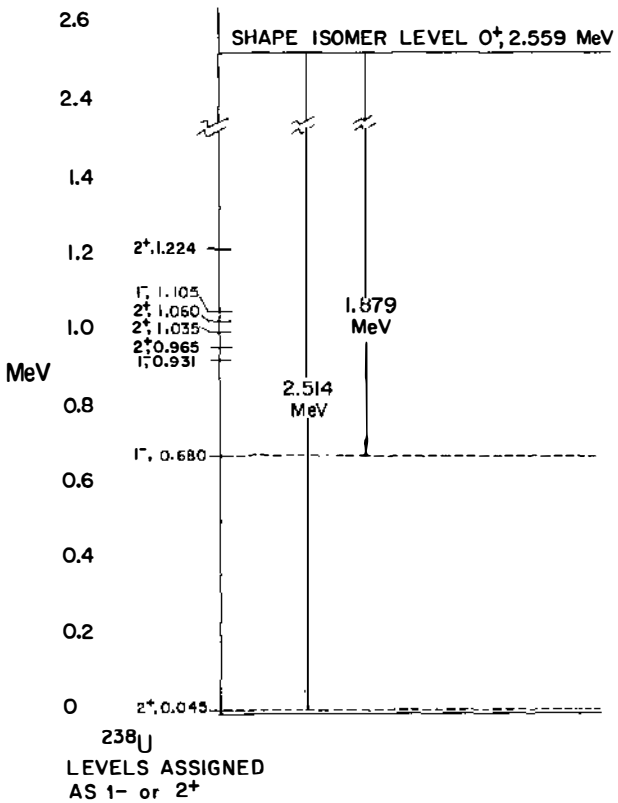

Figure 15 Decay scheme for the ^{238}U γ-branch based on the assumption that the 2.514-MeV transition is the decay of the shape-isomeric state to the first excited 2^+ state at 0.045 MeV in normally deformed ^{238}U. From Russo et al (13).

Annu. Rev. Nucl. Sci. 1977.27:1-35. Downloaded from www.annualreviews.org
Access provided by 2409:4070:4701:c29b:fcdc:51af:e256:c850 on 09/30/22. For personal use only.

in neutron capture has been studied in another experiment, and from the measured ratio of delayed to prompt fission, an indirect estimate of 7 ± 2 for the ratio of γ decay to fission decay of the isomer has been made (80).

Although a γ branch has not been detected in any odd-A nuclei, it is believed that the failure to observe even-odd uranium isomers is a consequence of γ decay being the predominant mode of decay for these isomers. Similarly, the paucity of isomers for neptunium isomers and the very low yield of the one known isomer (81a) suggest that γ decay is predominant for the neptunium shape isomers as well.

Bowman (81b) has suggested that additional information about the barrier penetrabilities can be determined from measurements of photo-fission cross sections at very low energy, where a shelf in the photo-fission cross section is expected. Evidence for such a shelf has been seen in several nuclei (81c, 81d).

Fragment Kinetic Energy and Mass Distributions for Isomeric Fission

Differences between the fission characteristics of isomeric fission and either ground-state spontaneous fission or induced fission could arise from following different dynamical paths to scission depending on the initial excitation energy or depending

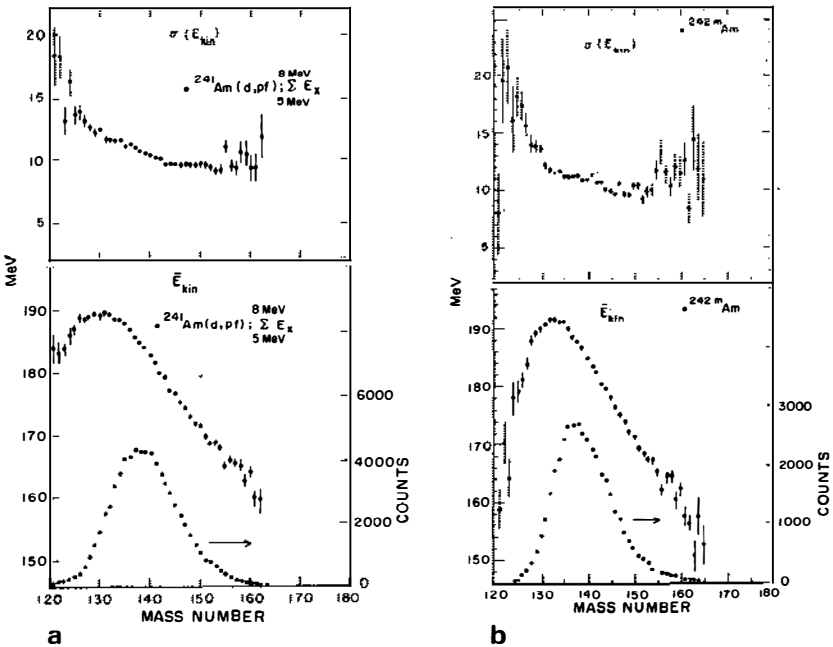

Figure 16 (*a*) The average total kinetic energy (*bottom*) and its standard deviation (*top*) as a function of the heavy fragment pre-neutron emission mass for the ^{241}Am(d,pf) reaction summed over the excitation energy region of 5–8 MeV in ^{242}Am. The bottom points in the figure show the relative mass-yield distribution for the ^{242}Am* fission. (*b*) The same quantities for ^{242m}Am isomeric fission. After Weber et al (85).

Annu. Rev. Nucl. Sci. 1977.27:1-35. Downloaded from www.annualreviews.org
Access provided by 2409:4070:4701:c29b:fcdc:51af:e256:c850 on 09/30/22. For personal use only.

on whether the nucleus starts at its ground-state deformation or its isomeric-state deformation. If the excitation-energy effect were dominant, one would expect values for isomer fission intermediate between those of ground-state and induced fission.

Early measurements (82, 83) of single-fragment kinetic energies for 14-msec ^{242m}Am isomeric fission showed a double-peaked kinetic energy distribution. This implied that the mass distribution for isomeric fission is asymmetric, as it is for ground-state spontaneous fission and for induced fission at low excitation energies. Ferguson et al (84) extended these studies to other isomers and found that both the mass distributions and total kinetic energy distributions are similar to those found for normal spontaneous and low-excitation energy fission. In a more recent experiment (85) a careful comparison between the properties of coincident fission fragments for isomeric and excited-state fission of ^{242}Am has been performed. The mass distributions deduced from these measurements are shown in the bottom parts of Figure 16, together with the dependence of the total kinetic energy on the mass of the heavy fragments. Also shown in the upper part of the figure is the dependence of the standard deviations of the kinetic energy distributions on mass number. The qualitative similarities between the two kinds of fissions is clear. There are some differences, however. The average value of the total kinetic energy for isomer fission is 2.0 ± 0.4 MeV larger than for the induced fission. (Another, less accurate experiment (86) gives an opposite result of -1.85 ± 0.84 MeV.) A larger energy compared to induced fission is opposite to the trend (87–89) in which spontaneous fission from the ground state is found to have a lower average total kinetic energy than that for thermal neutron-induced fission from the same compound nucleus. It is, however, consistent with the observation that the average total kinetic energy in induced fission decreases with excitation energy at energies near ($E^* = 4.8$–9 MeV) (90–92) and above (93) the barrier. Weber et al (94) have found that the average kinetic energy for isomeric fission of ^{240}Pu is larger than that for either spontaneous fission or near-barrier fission of the same nucleus, in agreement with the observations for ^{242}Am.

The peak-to-valley ratio for isomeric fission from ^{242}Am is larger than that for the higher-excitation energy fission (85). This may simply reflect the known tendency for the peak-to-valley ratio to decrease with increasing excitation energy, or it may indicate a tendency to follow slightly different trajectories for through-the-barrier fission starting from the isomeric state as compared to over-the-barrier fission starting from the ground-state deformation.

EXCITATIONS OF SHAPE ISOMERS

Rotational Excitations

The lowest-lying states of normally deformed even-even nuclei are rotational states, with the lowest state occurring at an energy more than an order of magnitude smaller than the lowest-lying vibrational or two-quasiparticle states. For the more highly deformed shape-isomeric state, the rotational excitations will occur at even lower energies due to the larger moment of inertia. Rotational bands in two even-even shape-isomer nuclei have been identified, as has been discussed earlier in connection

Annu. Rev. Nucl. Sci. 1977.27:1-35. Downloaded from www.annualreviews.org
Access provided by 2409:4070:4701:c29b:fcdc:51af:e256:c850 on 09/30/22. For personal use only.

with moments of inertia. The rotational spacings for these isomers are indeed less than half the spacings for rotational bands based on the normally deformed ground state. If the rotational energies are represented as a power series in the angular momentum

$$E(J) = aJ(J+1) + bJ^2(J+1)^2, \qquad 9.$$

the coefficient b of the second correction term is much smaller for the isomer than for the ground state, as can be seen in Figure 8. This result can be qualitatively understood as a consequence of a better separation between the rotational degree of freedom and other degrees of freedom, such as vibrations and particle excitations, when the rotational energies are very low, as for the shape isomeric state. If the correction term is attributed to centrifugal stretching, it has been shown (32) that one can deduce the ratio of the stiffness in the two wells, $C_{\mathrm{I}}/C_{\mathrm{II}}$ from the ratio of the values of the b coefficients in the above expression, if one makes the assumption that the dependence of the moment of inertia on deformation has the same functional dependence at the first and second minima. This assumption, however, is quite questionable in view of the significant modulations in the dependence of the microscopically calculated moments of inertia on deformation (see Figure 9).

An alternative expansion of the rotational energies in even powers of the rotational frequency (95), rather than angular momentum, gives coefficients for the second term that are within their errors the same for the ground-state and isomeric-state bands (10). This is consistent with our earlier analysis, as it can be shown that this model is equivalent to the VMI model and that the coefficient of this term depends only on the stiffness C and not on the deformation (96).

Theoretical calculations indicate that the stiffness at the first and second minima are comparable. The potential energy function for ^{240}Pu of Tsang & Nilsson (77) is approximately twice as stiff at the first minimum as at the second minimum. The potential energy surface of Ledergerber & Pauli (72) yields a slightly larger stiffness at the first minimum than at the second minimum.

Vibrational Excitations

There is no experimental information on the low-lying vibrational states at the second minimum. An approximate estimate of the expected vibrational-level spacings can be obtained by using the dependence of $\hbar\omega$ on the stiffness C and the inertial parameter B, $\hbar\omega = (C/B)^{\frac{1}{2}}$, to scale the known values of $\hbar\omega$ at the first minimum, $\hbar\omega \sim 1$ MeV, to the second minimum. Goldstone et al (97) have deduced a value of $\hbar\omega_{\mathrm{II}}/\hbar\omega_{\mathrm{I}} = 0.5$ for ^{240}Pu from the calculations of Ledergerber & Pauli (72). A somewhat larger value is indicated by the calculation of Randrup et al (74). Dudek (98) has calculated the transmission resonances for ^{241}Pu from potential and inertial functions resulting from a microscopic theoretical calculation. This calculation indicates that $\hbar\omega = 0.8$ MeV.

Although the lowest vibrational states are not known, there is information on higher vibrational states from the observation of resonances in the sub-barrier fission cross-sectional excitation functions for neutron, photon, and direct-reaction charged-particle–induced fission. Transmission resonances are expected to occur at

Annu. Rev. Nucl. Sci. 1977.27:1-35. Downloaded from www.annualreviews.org
Access provided by 2409:4070:4701:c29b:fcdc:51af:e256:c850 on 09/30/22. For personal use only.

Annu. Rev. Nucl. Sci. 1977.27:1-35. Downloaded from www.annualreviews.org
Access provided by 2409:4070:4701:c29b:fcdc:51af:e256:c850 on 09/30/22. For personal use only.

energies closely corresponding to the collective β-vibrational levels of the shape isomer. These vibrations, sometimes designated fission vibrations, have $K^{\pi} = 0^{+}$ for even-even nuclei. Due to the strong dependence of the penetrability on energy relative to the barrier, only a few such resonances are likely to be experimentally observable. Additional resonances are expected, due to the presence of states that consist of a fission vibration coupled to other kinds of collective low-lying excitations such as rotations, $K = 2^{+}$ gamma vibrations, $K = 0^{-}$ octupole vibrations, etc. In simple models these states give rise to transmission resonances with strengths comparable to that for the $K = 0^{+}$ bandhead. For example, a strong resonance near 5-MeV excitation in ^{240}Pu (relative to the ground state) has been known for a long time (99–101). Angular correlation studies show that $K = 0$ fission channels are dominant for this resonance (102–104). The 5-MeV vibrational level is complex, with structures at 4.95 MeV and 5.1 MeV. In some analyses the weaker 4.95-MeV resonance is assumed to be $K = 0^{+}$, whereas in others the 5.1-MeV resonance is attributed to the $K = 0^{+}$ state. Less prominent structure has been seen at 5.25 and 5.45 MeV, and attributed (97, 105) to other collective states coupled to the 5-MeV vibrational state. The region below 5 MeV has been reinvestigated in more detail recently, revealing two peaks at 4.55 and 4.70 MeV (97). Angular correlation measurements (106) again show that this region is dominated by $K = 0$. (Such measurements cannot, however, distinguish between $K = 0^{-}$ and $K = 0^{+}$ contributions.) Goldstone et al have proposed that the 4.55-MeV level is the $K = 0^{+}$ fission vibration and the 4.70-MeV level is a $K = 0^{-}$ collective excitation based on this level. This yields an energy difference of 0.4 or 0.55 MeV between two vibrational levels, depending on which resonance near 5 MeV is attributed to $K = 0^{+}$. (One would expect it to be the lower, but model calculations of the fission probability significantly overestimate the strength if it is taken to be 0^{+}.) These results would indicate $\hbar\omega_{II} \sim 0.4$ or 0.55. However, the next higher $K = 0^{+}$ resonance has not been observed, and comparison of model calculations (107) with the rather structureless data at higher energies suggest that it has to be above 5.8 MeV in excitation energy. This is rather surprising, as one would expect anharmonic effects to make the spacing smaller rather than larger as one approaches the top of the barrier. The conclusion that there is no 0^{+} resonance between 5.0 and 5.8 MeV has to be taken as somewhat tentative, as the same model calculations seriously overestimate the strength of the lower $K = 0^{+}$ resonance assumed to exist at 4.95 MeV. The very recent observation at Heidelberg (108) of a 4.21-MeV resonance with an anisotropy more indicative of a 0^{+} or 0^{-} resonance than the 4.55- and 4.70-MeV resonances further complicates the interpretation of these results. If the 4.2-MeV, rather than the 4.55-MeV, resonance is the first 0^{+} resonance below about 5 MeV, then $\hbar\omega_{II}$ would be about 0.8 MeV.

Single-Particle Excitations

ODD-A NUCLEI For a deformed heavy nucleus, the average spacing between single-particle levels is 200–300 keV (see Figure 7). If two such levels happen to differ in K by more than a few units, then the rate for γ decay from the upper level to the lower level may be sufficiently slow that the decay of this state can be observed as a

delayed fission component, either by virtue of a direct spontaneous-fission branch or as a result of γ decay to a lower state that then decays by spontaneous fission. In such circumstances one may expect to see two distinct fission half-lives. A number of such pairs of isomers have been observed in odd-A nuclei, as can be seen in Figure 11.

The most thoroughly studied pair of isomers is in ^{237}Pu. The longer-lived state has been found to lic 0.3 ± 0.15 MeV above the shorter-lived state (109). The spin of the upper state has been found to be higher than that of the short-lived state (44). Fragment angular distributions show that the upper state decays primarily directly by spontaneous fission rather than by spontaneous fission following γ decay to the lower-lying level. More quantitative information on the quantum numbers of the levels from angular distribution and g-factor measurements does not seem fully consistent at the present time. A resolution of this problem and the gathering of definitive information on other pairs would provide a valuable test of the theoretical single-particle level schemes shown in Figure 7.

TWO-QUASIPARTICLE EXCITATIONS There are now three even-even Pu isotopes and two even-even Cm isotopes for which two isomers are known. The isomer half-lives

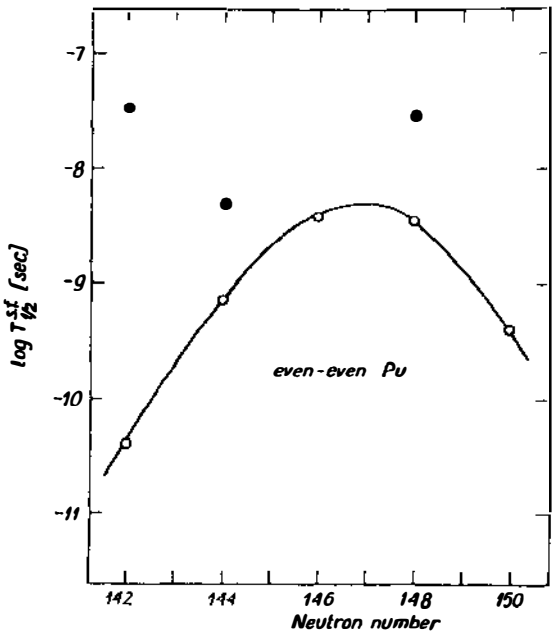

Figure 17 Logarithm of the half-lives for spontaneous fission from the shape-isomeric state in even-even Pu isotopes as a function of neutron number. Experimental points considered to represent the decay of the lowest state in the second minimum are connected by a solid curve [from (30)].

Annu. Rev. Nucl. Sci. 1977.27:1-35. Downloaded from www.annualreviews.org
Access provided by 2409:4070:4701:c29b:fcdc:51af:e256:c850 on 09/30/22. For personal use only.

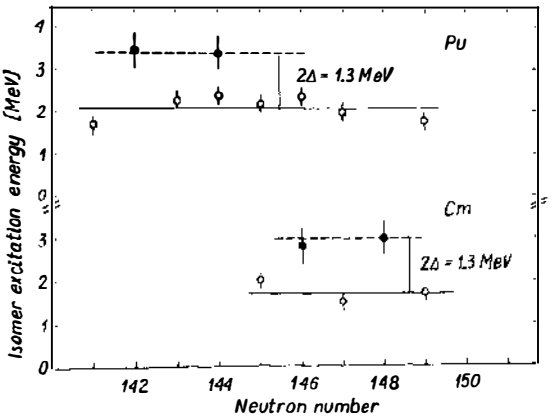

Figure 18 Excitation energies of isomeric states in Pu and Cm isotopes compared for ground states, open circles, and (presumably) two-quasiparticle states, closed points [from (29)].

for the even-even Pu isomers are plotted versus number in Figure 17. The isomers plotted with open circles have shorter half-lives, which vary smoothly with neutron number and have been attributed to the lowest state in the second minimum. The longer-lived states are attributed to two-quasiparticle excitations. In the case of ^{238}Pu there is direct experimental support for this view. The long-lived isomer has a threshold 1.3 MeV higher than the shorter-lived isomer and is also formed in lower yield (65). There are also short-lived isomers in ^{236}Pu and in ^{242}Cr and ^{244}Cm, which have excitation energies about 1.3 MeV higher than their neighboring odd-A isomers, as illustrated in Figure 18. An excitation energy of 1.3 MeV is very similar to that of two-quasiparticle excitations of ground-state plutonium and curium nuclei. This result does not allow us to determine whether the pairing strength G is independent of deformation. Some theoretical calculations of potential energy surfaces, moments, and inertial parameters have been performed, both with G constant and with G proportional to the surface area. Pairing theory predicts a dependence intermediate to these assumptions (110). In the latter case of G proportional to the surface area, one would expect two-quasiparticle excitations to be about 0.3 MeV greater at the second minimum than at the first minimum.

Another piece of experimental evidence that the longer-lived isomers are not the spin-zero ground states of the second minimum comes from anisotropy measurements discussed earlier. Both 30-nsec ^{236}Pu and 6-nsec ^{238}Pu have anisotropies deviating significantly from unity (see Table 1), with the sign of the deviation indicating that $K_b \approx I$. More quantitative statements about the spin of these states cannot be made at the present time. If these two-quasiparticle states were to have significant branching ratios to the ground state of the second minimum, then a determination of the population of the rotational levels could lead to unambiguous spin determinations.

Annu. Rev. Nucl. Sci. 1977.27:1-35. Downloaded from www.annualreviews.org
Access provided by 2409:4070:4701:c29b:fcdc:51af:e256:c850 on 09/30/22. For personal use only.

Annu. Rev. Nucl. Sci. 1977.27:1-35. Downloaded from www.annualreviews.org
Access provided by 2409:4070:4701:c29b:fcdc:51af:e256:c850 on 09/30/22. For personal use only.

CONCLUSION

During the last few years, the study of spontaneous fission isomers has come of age. The survey experiments defining the systematics of half-lives, excitation energies, and barrier parameters have been largely completed. The emphasis in recent years has been on more quantitative and spectroscopic aspects of shape isomerism. The evidence for spontaneous-fission isomers being shape isomers with a deformation more than twice that of the ground states has been firmly established with the determination of the moment of inertia and of the electric quadrupole moment of several isomers. A start has been made on the determination of spectroscopic properties of shape isomers, such as spins and moments. These experiments are very difficult and a number of ingenious methods are being developed and applied.

Our theoretical understanding of shape isomerism is in fairly good condition. There are, however, several areas where significant discrepancies between theory and experiment persist. Whether these are quantitative or qualitative remains to be seen. One of the more interesting theoretical developments has been the demonstration of the importance of inertial as well as potential energy effects on the dynamical path from the ground or isomeric state toward the scission point. Comparison of spins and moments with theoretical calculations should improve the definition of the single-particle potential and allow for a more reliable extrapolation to other deformations and mass regions.

The possible manifestation of shape isomerism in other regions of the periodic table is an interesting area for future exploration. It is highly unlikely that states of such "pure" deformation and high stability as the spontaneously fissioning isomers will be encountered. The shape isomers in the actinide region have two factors going for them that are fairly unique. In the first place, the potential energy surface on which the shell effects play their game is unusually flat because of the near cancellation of the shape dependence of the surface and Coulomb energies. Second, the number of particles involved, and hence the effective mass, is large, inhibiting the mixing of states of rather different deformation. In spite of these unique aspects, it is quite likely that there are shape isomers with sufficient purity to manifest themselves in a number of ways. There is already some evidence for such states in such diverse situations as the $4p$-$4h$ states of ^{16}O and in the crossings of rotational bands with quite different deformations in the rare-earth region. The full relationship between these phenomena and spontaneously fissioning shape isomers remains to be revealed.

ACKNOWLEDGMENTS

I am indebted to P. Paul, J. Pedersen, R. Sielcmann, G. Sletten, H. J. Specht, and V. Metag for helpful comments and information about work in progress.

Annu. Rev. Nucl. Sci. 1977.27:1-35. Downloaded from www.annualreviews.org
Access provided by 2409:4070:4701:c29b:fcdc:51af:e256:c850 on 09/30/22. For personal use only.

Literature Cited

1. Polikanov, S. M., Druin, V. A., Karnaukhov, V. A., Mikheev, V. L., Pleve, A. A., Skobelev, N. K., Subbottn, V. G., Ter-Akopyan, G. M., Fomichev, V. A. 1962. *Sov. Phys. JETP* 15:1016
2. Swiatecki, W. J. 1964. *Nuclidic Masses*, p. 58. (Proc. Conf. Vienna 1963) Vienna: Springer-Verlag
3. Strutinsky, V.M. 1966. *Sov.J. Nucl. Phys.* 3:449
4. Strutinsky, V. M. 1967. *Nucl. Phys. A* 95: 420
5. Bjørnholm, S., Bohr, A., Mottelson, B. R. 1974. See Ref. 9, I:367
6. Brack, M., Damgaard, J., Pauli, H. C., Jensen, A. S., Strutinsky, V. M., Wong, C. Y. 1972. *Rev. Mod. Phys.* 44:320
7. Pauli, H. C. 1973. *Phys. Rev. C* 7:35
8. Möller, P., Nix, J. R. 1973. See Ref. 9, I:103
9. Physics and Chemistry of Fission 1973. Proc. Symp., Rochester, NY, August 13–17. Vol. I, Vol. II. Vienna: IAEA. 578 pp., 525 00.
10. Specht, H. J. 1974. *Rev. Mod. Phys.* 46: 773
11. Vandenbosch, R., Huizenga, J. R. 1973. *Nuclear Fission*, New York: Academic. 422 pp.
12. Britt, H. C., Bolsterli, M., Nix, J. R. 1973. *Phys. Rev. C* 7:801
13. Russo, P. A., Pedersen, J., Vandenbosch, R. 1975. *Nucl. Phys. A* 240:13
14. Back, B. B., Hansen, O., Britt, H. C., Garrett, J. D. 1974. *Phys. Rev. C.* 9:1924
15. Back, B. B., Britt, H. C., Hansen, O., Leroux, B., Garrett, J. D. 1974. *Phys. Rev. C* 10:1948
16. Bassichis, W. H., Tuerpe, D. R., Tsang, C. F., Wilets, L. 1973. *Phys. Rev. Lett.* 30:294
17. Brack, M., Quentin, P. 1973. See Ref. 9, I:231
18. Flocard, H., Quentin, P., Vautherin, D., Kerman, A. K. 1974. See Ref. 9, I:221
19. Möller, P., Nilsson, S. G. 1970. *Phys. Lett. B* 31:283
20. Pauli, H. C., Ledergerber, T., Brack, M. 1971. *Phys. Lett. B* 34:264
21. Pashkevich, V. V. 1971. *Nucl. Phys. A* 169:275
22. Mustafa, M. G., Mosel, U., Schmitt, H. W. 1972. *Phys. Rev. Lett.* 28:1050
23. Pashkevich, V. V. 1969. *Nucl. Phys. A* 133:400
24. Larson, S. E., Ragnarsson, I., Nilsson, S. G. 1972. *Phys. Lett. B* 38:269
25. Götz, U., Pauli, H. C., Junken, K. 1972. *Phys. Lett. B* 39:436
26. Schultheiss, H., Schultheiss, R. 1971. *Phys. Lett. B* 34:245
27. Möller, P., Nix, J. R. 1974. *Nucl. Phys. A* 229:269
28. Larsson, S. E., Leander, G. 1973. See Ref. 9, I:177
29. Specht, H. J. 1975. *Nukleonika* 20:717
30. Metag, V. 1975. *Nukleonika* 20:789
31. James, G. D., Lynn, J. E., Earwaker, L. G. 1972. *Nucl. Phys. A* 189:225
32. Vandenbosch, R. 1974. See Ref. 9, I:251
33. Pauli, H. C., Ledergerber, T. 1971. *Nucl. Phys. A* 175:145
34. Möller, P. 1972. *Nucl. Phys. A* 192:529
35. Specht, H. J., Konecny, E., Weber, J., Kozhuharov, C. 1973. See Ref. 9, I:285
36. Galeriu, D., Marinescu, M., Poenaru, D., Vilcov, I., Vilcov, N. 1974. See Ref. 9, I:297
37. Kalish, R., Herskind, B., Pedersen, J., Shackleton, D., Strabo, L. 1974. *Phys. Rev. Lett.* 32:1009
38. Konecny, E. 1975. Private communication as quoted by P. Z. Hien, 1976. *Sov. J. Nucl. Phys.* 22:489
39. Shackleton, D., Herskind, B., Kalish, R., Pedersen, J., Strabo, L. 1974. *Proc. Int. Conf. Hyperfine Interactions Studied Nucl. React. Decay*, ed. E. Karlson, R. Wappling, 3:28–74. Amsterdam: North-Holland
40. Habs, D., Jaeschke, E., Just, M., Metag, V., Neumann, B., Repnow, R., Singer, P., Specht, H. J. 1974. Max Planck Inst. Kernphys., Jahresbericht, 1974. p. 1
41. Metag, V., Habs, D., Specht, H. J., Ulfert, G., Kozhuharov, C. 1976. *Hyperfine Interactions* 1:405
42. Hamamoto, I., Ogle, W. 1975. *Nucl. Phys. A* 240:54
43. Hien, P. Z. 1976. *Sov. J. Nucl. Phys.* 22:489
44. Russo, P. A., Vandenbosch, R., Mehta, M., Tesmer, J. R., Wolf, K. L. 1971. *Phys. Rev. C* 3:1595
45. Mosel, U., Schmitt, H. W. 1971. *Nucl. Phys. A* 165:13
46. Bohr, A., Mottelson, B. R. 1975. *Nuclear Structure*, Reading, Mass: Benjamin 2:228
47. See Ref. 46, p. 303
48. Nagamiya, S. 1972. Sci. Pap. Inst. Phys. Chem. Res. (Jpn) 66:39–140
49. Specht, H. J., Weber, J., Konecny, E., Heunemann, D. 1972. *Phys. Lett. B* 41:43
50. Borggreen, J., Pedersen, J., Sletten, G., Heffner, R., Swanson, E. 1977. *Nucl. Phys A* 279:189

Annu. Rev. Nucl. Sci. 1977.27:1-35. Downloaded from www.annualreviews.org
Access provided by 2409:4070:4701:c29b:fcdc:51af:e256:c850 on 09/30/22. For personal use only.

51. Griffin, J. J., Rich, M. 1960. *Phys. Rev.* 118:850
52. Damgaard, J., Pauli, H. C., Strutinsky, V. M., Wong, C. Y., Brack, M., Stenholm-Jensen, A. 1969. IAEA Symp. Phys. Chem. Fission, 2nd, IAEA, Vienna, p. 213
53. Krumlinde, J. 1971. *Nucl. Phys. A* 160: 471
54. Sobiczewski, A., Bjørnholm, S., Pomorski, K. 1973. *Nucl. Phys. A* 202: 274
55. Brack, M., Ledergerber, T., Pauli, H. C., Jensen, A. S. 1974. *Nucl. Phys. A* 234: 185
56. Hamamoto, I. 1975. *Phys. Lett. B* 56:431
57. See Ref. 11, p. 40
58. Habs, D., Metag, V., Specht, H. J., Ulfert, G. 1977. *Phys. Rev. Lett.* 38:387
59. Metag, V., Sletten, G. 1977. *Nucl. Phys. A* 282:77
60. Pomorska, B. N., Sobiczewski, A., Pomorski, K., *Proc. Int. Conf. Nucl. Phys., Munich, 1973.* I:598
61. Nerlo-Pomorska, B. 1976. *Nucl. Phys. A* 259:481
62. Metag, V., Liukkonen, E., Sletten, G., Glomset, O., Bjørnholm, S. 1974. *Nucl. Instrum. Methods* 114:445
63. Metag, V., Liukkonen, E., Glomset, O., Bergman, A. 1974. See Ref. 9, p. 317
64. Christiansen, J., Hempel, G., Ingwersen, H., Klinger, W., Schatz, G., Schatz, G., Withurn, W. 1975. *Nucl. Phys. A* 239: 253
65. Limkilde, P., Sletten, G. 1973. *Nucl. Phys. A* 199:504
66. Sletten, G., Metag, V., Liukkonen, E. 1976. *Phys. Lett. B* 60:153
67. Britt, H. C. 1973. *At. Nucl. Data Tables* 12:407
68. See Ref. 11, p. 54
69. Urin, M. G., Zaretsky, D. F. 1966. *Nucl. Phys.* 75:101
70. Sobiczewski, A., Szymanski, Z., Wycech, S. 1969. *Second IAEA Symposium Phys. Chem. Fission, Vienna, Austria,* p. 905
71. Sobiczewski, A., *Proc. Robert A. Welch Found. Conf. Chem. Res., Houston,* p. 13. Houston: Robert A. Welch Found.
72. Ledergerber, T., Pauli, H. C. 1973. *Nucl. Phys. A* 207:1
73. Pauli, H. C., Ledergerber, T. See Ref. 9, I:463
74. Randrup, J., Larsson, S. E., Möller, P., Nilsson, S. G., Pomorski, K., Sobiczewski, A. 1976. *Phys. Rev. C* 13: 229
75. Wilets, L. 1964. *Theories of Nuclear Fission,* Oxford: Clarendon
76. Nix, J. R., Walker, G. E. 1969. *Nucl. Phys. A* 132:60
77. Tsang, C. F., Nilsson, S. G. 1970. *Nucl. Phys. A* 140:275
78. Russo, P. A., Pedersen, J., Vandenbosch, R. 1974. See Ref. 9, I:271
79. Habs, D., Just, M., Metag, V., Mosler, E., Neumann, B., Paul, P., Singer, P., Specht, H. J., Ulfert, G. 1975. Max Planck Inst. Kernphys., Jahresbericht, p. 55
80. Andersen, V., Christensen, C. J., Borggreen, J. 1976. *Nucl. Phys. A* 269:338
81a. Wolf, K. L., Unik, J. P. 1973. *Phys. Lett. B* 43:25
81b. Bowman, C. D. 1975. *Phys. Rev. C* 12: 856
81c. Bowman, C. D., Schröder, I. G., Dick, C. E., Jackson, H. E. 1975. *Phys. Rev. C* 12:863
81d. Zhuchko, V. E., Ignatyuk, A. V., Ostapenko, Yu. B., Smirenkin, G. N., Soldatov, A. S., Tsipen uk, Yu. M. 1975. *JETP Lett.* 22:118
82. Brenner, D. S., Westgaard, L., Bjørnholm, S. 1966. *Nucl. Phys.* 89:267
83. Erkkila, B. H., Leachman, R. B. 1968. *Nucl. Phys. A* 108:689
84. Ferguson, R. L., Plasil, F., Alam, G. D., Schmitt, H. W. 1971. *Nucl. Phys. A* 172: 33
85. Weber, J., Erdal, B. R., Gavron, A., Wilhelmy, J. B. 1976. *Phys. Rev. C* 13: 189
86. Fontenla, C. A., Fontenla, D. P. 1973. *Proc. Int. Conf. Nucl. Phys., Munich,* ed. J. DeBoer, H. J. Mang, I:588. Amsterdam: North-Holland & Am. Elsevier
87. Okolovich, V. N., Smirenkin, G. N. 1963. *Sov. Phys. JETP* 16:1313
88. Unik, J. P., Gindler, J. E., Glendenin, L. E., Flynn, K. F., Gorski, A., Sjoblom, R. K. 1974. See Ref. 9, II:19
89. Deruytter, A. J., Wegener-Penning, G. 1974. *Physics and Chemistry of Fission 1973,* 2:51. Vienna: IAEA
90. Unik, J. P., Loveland, W. D. 1971. Private communication quoted in Ref. 11, p. 300
91. Akimov, N.I., Vorobeva, V. G., Kabenin, V. N., Kolosov, N. P., Kuzminov, B. D., Sergachev, A. I., Smirenkina, L. D., Tarasko, M. Z. 1971. *Sov. J. Nucl. Phys.* 13:272
92. Milton, J. C. D., Fraser, J. S., Specht, H. J. 1977. *Proc. Eur. Conf. Nucl. Phys., Aix-en-Provence, 1972,* Pap. I–15
93. Ferguson, R. L., Plasil, F., Pleasanton, F., Burnett, S. C., Schmitt, H. W. 1973. *Phys. Rev. C* 7:2510
94. Weber, J., Specht, H. J., Konecny, E.,

Heunemann, D. 1974. *Nucl. Phys. A* 221:414
95. Harris, S. M. 1965. *Phys. Rev. B* 138: 509
96. Mariscotti, M. A. I., Scharff-Goldhaber, G., Buck, B. 1969. *Phys. Rev.* 178:1864
97. Goldstone, P. D., Hopkins, F., Malmin, R. E., von Brentano, P., Paul, P. 1976. *Phys. Lett. B* 62:280
98. Dudek, J. 1973. *Nucl. Phys. A* 203:121
99. Pedersen, J., Kuzminov, B. D. 1969. *Phys. Lett. B* 29:176
100. Britt, H. C., Burnett, S. C., Cramer, J. D. 1969. *Proc. IAEA Symp. Phys. Chem. Fission, 2nd, Vienna,* p. 375. Vienna:IAEA
101. Specht, H. J., Fraser, J. S., Milton, J. C. D., Davies, W. G. 1969. See Ref. 100, p. 363
102. Britt, H. C., Gibbs, W. R., Griffin, J. J., Stokes, R. H. 1965. *Phys. Rev. B* 139: 354
103. Specht, H. J., Fraser, J. S., Milton, J. C. D. 1966. *Phys. Rev. Lett.* 17:1187
104. Britt, H. C., Rickey, F. A. Jr., Hall, W. S. 1968. *Phys. Rev.* 175:1525
105. Back, B. B., Bondorf, J. P., Otroshenko, G. A., Pedersen, J., Rasmussen, B. 1969. See Ref. 100, p. 375
106. Glässel, P., Rösler, H., Specht, H. J. 1976. *Nucl. Phys. A* 256:220
107. Goldstone, P., Hopkins, F., Malmin, R. E., Paul, P. To be published
108. Just, M., Habs, D., Metag, V., Paul, P., Specht, H. J., Weber, J. 1976. Private communication
109. Vandenbosch, R., Russo, P. A., Sletten, G., Mehta, M. 1973. *Phys. Rev. C* 8: 1080
110. Kennedy, R. C., Wilets, L., Henley, E. M. 1964. *Phys. Rev. Lett.* 12:36

Annu. Rev. Nucl. Sci. 1977.27:1-35. Downloaded from www.annualreviews.org
Access provided by 2409:4070:4701:c29b:fcdc:51af:e256:c850 on 09/30/22. For personal use only.